The TOR signaling pathway regulates vegetative development, aflatoxin biosynthesis and pathogenicity in *Aspergillus flavus*

Guoqi Li, Xiaohong Cao, Elisabeth Tumukunde, Qianhua Zeng, Shihua Wang*

Key Laboratory of Pathogenic Fungi and Mycotoxins of Fujian Province, Key Laboratory of Biopesticide and Chemical Biology of Education Ministry, and School of Life Sciences, Fujian Agriculture and Forestry University, Fuzhou, 350002, China.

Corresponding author:
Name: Shihua Wang Professor
School of Life Sciences, Fujian Agriculture and Forestry University
Fuzhou, Fujian Province, 350002, China
Phone/Fax: +86-591-83787126
E-mail: wshyyl@sina.com

These authors contributed equally to this work.

Abstract

The target of the rapamycin (TOR) signaling pathway is highly conserved and important in eukaryotes. It is involved in the regulation of various biological processes. However, systematic studies on this pathway in the genus *Aspergillus* have not been reported. Here, we identified and characterized nine genes encoding components of the TOR pathway in *A. flavus*, and investigated their biological, genetic and biochemical functions. The FK506-binding protein FKBP3 and its lysine succinylation are important for aflatoxin production and rapamycin resistance. The Tor kinase plays a central role in the global regulation of growth, spore production, aflatoxin biosynthesis and rapamycin stress. As a major downstream effector molecule of Tor kinase, the Sch9 kinase might regulate the calcium and osmotic stress, AFB_1 synthesis of *A. flavus* by its S_TKc, S_TK_X domains and ATP binding site at K340. We also showed that Sch9 kinase might mediate crosstalk between the TOR and the HOG signaling pathways. TapA and TipA, the other downstream components of Tor kinase, play important roles in regulating mycelial growth and sclerotia formation in *A. flavus*. The member of the TapA-phosphatase complexes Sit4 and Ppg1 are important for hyphal development, sexual reproduction, sclerotia formation, AFB_1 biosynthesis, activation of the CWI and TOR signaling pathways in *A. flavus.* In addition, the another phosphatase complex Nem1/Spo7 play critical role in vegetative growth, conidiation, aflatoxin and LD biogenesis. This study provide new insights into constructing the regulatory network of the TOR signaling pathway and

revealing the molecular mechanism of the pathogenicity in *A. flavus*.

Keywords: The TOR signaling pathway; *Aspergillus flavus*; aflatoxin; vegetative development

Introduction

A. flavus is one of the most important phytopathogenic fungi species, which frequently contaminates various plants, causing economic losses in agricultural commodities and posing serious health concerns in developing countries [1]. *A. flavus* is also an opportunistic human pathogenic fungus that can cause aspergillosis in immune-compromised patients [2]. Aflatoxins (AFs), the toxic and carcinogenic secondary metabolites produced by *A. flavus*, are the most potent carcinogen present in nature, causing liver cancer in humans and animals [3]. Although most of the enzymatic reactions involved in AF biosynthesis have been elucidated and the genes encoding these enzymes have been isolated [4], the signaling pathway network and specific regulatory processes involved in AF biosynthesis are still unclear. Therefore, exploring the regulatory mechanism of the AF biosynthesis signaling pathway would provide new insights for preventing *A. flavus* and aflatoxins contamination.

In eukaryotes, the target of the rapamycin (TOR) signaling pathway is highly conserved and plays essential roles in several important biological processes, such as ribosome biosynthesis, cell growth and autophagy [5]. Several studies have shown that the TOR signaling pathway interacts with other signaling pathways (MAPK, CWI),

67 and they crosstalk to form a complex metabolic network to regulate cellular processes
68 [6-9]. The serine/threonine-protein kinase Tor acts as a crucial protein element in the
69 TOR signaling pathway, which interacts with other proteins to form multiprotein
70 complexes. There are two TOR complexes named TORC1 and TORC2 in
71 *Saccharomyces cerevisiae* [10]. TORC1-mediated signaling controls cell growth by
72 regulating many growth-related processes and is sensitive to rapamycin, while
73 TORC2-mediated signaling is mainly responsible for cytoskeletal remodeling and is
74 insensitive to rapamycin [11]. However, most organisms, including plants, animals and
75 filamentous fungi, have a single Tor kinase [12-13].

76 In the fungal kingdom, most studies on the TOR signaling pathway have been
77 conducted in budding yeast *S. cerevisiae* [14-15], and fission yeast *Schizosaccharomyces*
78 *pombe* [6.16-17]. In *S. cerevisiae*, rapamycin forms a complex with the peptidylprolyl
79 cis/trans isomerase FKBP12, which binds and inhibits Tor kinase. The Tap42
80 phosphatase complex is the main target of Tor kinase, and the Tap42 protein interacts
81 with the Tip41 protein to jointly regulate phosphatases such as Pp2A and Sit4.
82 Phosphatase Sit4 can dephosphorylate transcription factor GLN3, regulating the
83 nitrogen source metabolism pathway [18-19]. In addition, the other immediate effector
84 of TORC1 is AGC kinase Sch9, which participates in other cellular functions
85 including ribosome biosynthesis [20]. In filamentous fungi, the TOR signaling pathway
86 has been reported in *Fusarium graminearum* [21-22], *Magnaporthe oryzae* [23],
87 *Phanerochaete chrysosporium* [24], *Podospora anserine* [25], *A. nidulans* [26], *A.*
88 *fumigatus* [51-52], *F. fujikuroi* [27], *Botrytis cinerea* [28], *F. oxysporum* [29]and *Mucor*

89 *circinelloides* [30]. In a word, filamentous fungi TOR signaling branch mediates spatial
90 and temporal control of cell growth by activating anabolic processes such as ribosome
91 biosynthesis, lipid droplet biogenesis, carbon and nitrogen metabolism, protein, lipid,
92 and nucleotide synthesis, and repressing catabolic processes such as autophagy and
93 apoptosis.

94 In yeast and filamentous fungi, the TOR signaling pathway modulates cell growth
95 and vegetative differentiation by sensing changes in external nutrients, energy and
96 stress [31]. While the underlying mechanisms of multiple crosstalks between TOR and
97 the other signaling pathway in *A. flavus* pathogens are unclear. Therefore, we intented
98 to identify the gene of TOR signaling pathway and demonstrate their roles and
99 contributions in the regulation of vegetative development and aflatoxin biosynthesis
100 in *A. flavus*. In this study, the results indicated that the TOR signaling pathway plays
101 crucial roles in various cellular processes including vegetative development, aflatoxin
102 biosynthesis and pathogenicity in *A. flavus*. Our results also indicated a highly
103 complicated cross-regulatory relationship between TOR and other signaling pathways
104 (MAPK, CWI) that maintain cellular growth and survival in response to
105 environmental stress in *A. flavus*.

106 Results

107 Rapamycin inhibits *A. flavus* growth, sporulation, sclerotia and aflatoxin
108 production

109 Rapamycin, a secondary metabolite produced by *Streptomyces hygroscopicus*, is

110 useful in the inhibition of certain filamentous fungi. In *F. graminearum*, rapamycin
111 exhibited a strong inhibitory effect on growth and asexual reproduction [21], which
112 also induces lipid droplet (LD) accumulation in *F. graminearum* and other
113 filamentous fungi [22]. To investigate the effect of rapamycin on vegetative
114 development, secondary metabolism and LD accumulation of *A. flavu*s, we assayed
115 the sensitivity of the WT strain to rapamycin. We found that the *A. flavus* WT strain
116 was very sensitive to rapamycin, and the mycelial growth, the germination of dormant
117 spores and conidia formation of the WT strain were significantly inhibited on PDA
118 solid plates supplemented with 100 ng/mL rapamycin (**Fig. 1A**). The radial growth
119 and the spore production of *A. flavus* WT strain were gradually decreased with the
120 increasing concentration of rapamycin(**Fig. 1D,1F**). In addition, the rapamycin also
121 showed intense inhibition on sclerotia and AFB_1 biosynthesis. As shown in **Fig. 1B**
122 and **1C**, compared to untreated strains, *A. flavus* was unable to synthesize aflatoxin
123 and form sclerotia in PDA added with 100 ng/mL rapamycin. Furthermore, we
124 observed that *A. flavus* displayed a dramatic reduction in the rate of spore germination
125 and sparser conidiophores with rapamycin treatment (**Fig. S2A,S2B**). Calcofluor
126 white is a chemifluorescent blue dye that is nonspecifically used to bind to the chitin
127 of fungi. Fluorescence microscopy showed that the blue fluorescence on the cell wall
128 is significantly diminished when treated with rapamycin (**Fig. S2C**). The intracellular
129 lipid droplets were stained by BODIPY in the hyphae, and we found that the hyphae
130 treated with rapamycin contained many more LDs (**Fig. 9A**). These findings
131 suggested that rapamycin-treated hyphae led to the accumulation of LD biogenesis

132 and reduction of chitin content. To explore the potential regulatory function of the
133 TOR pathway to affect the growth, sporulation, sclerotia and aflatoxin biosynthesis of
134 *A. flavu*s, qRT-PCR was used to determine the expression levels of genes related to
135 conidia, sclerotia and aflatoxin biosynthesis. The transcription levels of sporulation
136 and sclerotia genes were both significantly downregulated in rapamycin treatment
137 strains, while the genes related to aflatoxin synthesis were almost not expressed(**Fig.**
138 **1G-1I**), which indicated that the TOR pathway is involved in growth, sporulation,
139 sclerotia and aflatoxin biosynthesis in *A. flavu*s by regulating these genes. All the
140 above results showed that rapamycin affects the growth, sporulation, sclerotia and
141 aflatoxin synthesis of *A. flavus*, indicating that the TOR pathway plays important roles
142 in vegetative growth and secondary metabolism in *A. flavus*.

143 **Effect of FKBP3 and its lysine succinylation on AFB_1 biosynthesis and**
144 **rapamycin resistance in *A. flavus***

145 FK506-binding proteins (FKBPs) are highly conserved immunophilin family and
146 its members involved in various cellular functions including protein folding,
147 immunosuppression, signaling transduction and transcription[33]. FKBPs act as
148 molecular switches, which elicit function through binding and altering the
149 conformation of target proteins. In *S. cerevisiae*, FKBP12 and rapamycin form a
150 complex that negatively regulates the Tor kinase activity[33]. According to the protein
151 sequence of peptidylprolyl isomerase fprA from *A. nidulans*. Four genes encoding
152 putative proteins with FK506 binding domain, named *FKBP1*(AFLA_126880) ,
153 *FKBP2*(AFLA_087480), *FKBP3* (AFLA_010910) and *FKBP4*(AFLA_128200) were

154 identified from the *A. flavus* genome. These FKBPs contain a single FKBP-type
155 peptidylprolyl cis-trans isomerase conserved domain. Disruption strains for each
156 FKBP gene were generated by homologous recombination using the fusion PCR
157 approach. All FKBP disruption strains were confirmed by PCR and sequencing
158 analysis. Morphological analyses showed that mycelial growth and conidia formation
159 of all the FKBP mutants were similar to that of the WT strain on the PDA medium,
160 suggesting that FKBPs had no significant effects on the vegetative development (**Fig.**
161 **2A**). However, the number of sclerotia was significantly reduced in all FKBP mutants
162 compared to that of the WT strain (**Fig. S3**), indicating that FKBPs were essential for
163 sclerotia formation. We also assessed AFB_1 production via thin layer chromatography
164 (TLC), and the results showed that the deletion of FKBP3 led to an obvious decrease
165 in AFB_1 production compared to that of the WT strain (**Fig. 2B**). Taken together, these
166 data indicated that FKBPs are involved in sclerotia and aflatoxin biosynthesis in *A.*
167 *flavus*.

168 We found that the *A. flavus* WT strain was very sensitive to rapamycin. To
169 determine which FKBP is involved in rapamycin sensitivity, all mutants were cultured
170 in the PDA solid plates supplemented with 100 ng/mL rapamycin. The FKBP3
171 disrupted strain showed high resistance to rapamycin, but the FKBP1, FKBP2 and
172 FKBP4 deletion mutants showed no change in resistance to rapamycin (**Fig. 2A**).
173 These results demonstrated that FKBP3, rather than FKBP1, FKBP2 and FKBP4, is a
174 major target for rapamycin in *A. flavus*. For FK506-sensitivity analysis, we found that
175 mycelial growth and conidia formation of *A. flavus* were severely inhibited on PDA

176 added with 10 ng/mL FK506, and the deletion of FKBP3 resulted in increased
177 resistance of *A. flavu*s to FK506 compared to WT strain (**Fig. 2A**), indicating that the
178 FKBP3 was mainly involved in the regulation of FK506 resistance.

179 In a previous study, we accomplished a global succinylome analysis of *A. flavus*
180 [60]. Based on our succinylome result, we identified six reliable succinylation sites (K5,
181 K19, K40, K42, K55, K65) on FKBP3. Further evolutionary conservation analysis
182 revealed that lysine at 19 of FKBP3 was highly conserved in the *A. flavus* orthologs,
183 suggesting that this residue of FKBP3 may be important for an evolutionarily
184 conserved function, which may play a crucial role in regulating aflatoxin biosynthesis
185 in *A. flavus*. To these succinylation sites, the site-directed mutations were constructed
186 according to the homologous recombination strategy. Compared with the *A. flavus*
187 WT strain, all point mutants exhibited similar phenotype in vegetative growth and
188 conidiation. Interestingly, we observed that K19A displayed increased resistance to
189 rapamycin, and AFB_1 production was significantly reduced when compared to the WT
190 strain (**Fig. 3E, 3G**), suggesting an essential role of K19 succinylation of FKBP3 in
191 rapamycin resistance and aflatoxin biosynthesis. In addition, other point mutants,
192 including K40A, K42A and K55A, produced less AFB_1 compared to the WT strain
193 (**Fig. 3G**), illustrating that the succinylation of FKBP3 on others site are involved in
194 AF biosynthesis in *A. flavus*. However, the K19 site likely plays a more prominent
195 role than others sites in FKBP3 succinylation.

196 **Tor kinase plays important roles in *A. flavus***

197 In *S. cerevisiae*, the FKBP12 and rapamycin forms a gain-of-function complex

198 interacts specifically with the TOR proteins. The Tor kinases can bind to various
199 proteins to form complexes such as TORC1 and TORC2. TORC1 can sense signals
200 such as nutrients, growth factors, and stress in the environment, and participate in the
201 regulation of signaling pathways such as gene transcription, protein translation,
202 ribosome synthesis and autophagy[48]. To identify the ortholog of the *S. cerevisiae*
203 TOR in *A. flavus*, the *S. cerevisiae* TOR protein was used as search queries by BLAST
204 (https://blast.ncbi.nlm.nih.gov/Blast.cgi) in the *A. flavus* genome databasein. The *A.*
205 *flavus* genome has a single Tor kinase ortholog (AFLA_044350) encoding a protein
206 with 48.91% similarity to *S. cerevisiae* TOR2. To determine the function of Tor kinase
207 in *A. flavu*s, we targeted *Tor* for gene deletion. While we failed to obtained a null
208 mutant, we constructed a single copy deletion strain Δ*Tor1*$^{+}$/*Tor*2^{-} (containing one
209 copy of the *Tor* gene) constructed by homologous recombination. Compared with the
210 WT strain, the Δ*Tor1*$^{+}$/*Tor*2^{-} strain grew significantly slower on PDA (**Fig. 3C**), and
211 produced fewer conidia and sclerotia than the WT strain (**Fig. 3B,S4**). The results
212 from TLC showed that AFB_1 production of the Δ*Tor1*$^{+}$/*Tor*2^{-} strain was dramatically
213 decreased compared to that of WT strain (**Fig. 3F**). Furthermore, The qRT-PCR
214 results showed that the expression levels of the sexual sporulation and aflatoxin
215 synthesis genes were both downregulated in the Δ*Tor1*$^{+}$/*Tor*2^{-} mutant compared to
216 WT(**Fig. 3E,3H**). Interestingly, the Δ*Tor1*$^{+}$/*Tor*2^{-} strain cannot survive on PDA
217 amended with 100 ng/mL rapamycin (**Fig. 3C**). In addition, the Δ*Tor1*$^{+}$/*Tor*2^{-} strain
218 was more sensitive to osmotic stress and cell wall inhibitor, including NaCl, KCl,
219 CFW and CR (**Fig.S5**). These findings suggested that TOR is involved in vegetative

220 growth, asexual development, sclerotia formation, environmental stress and AF
221 biosynthesis in *A. flavus*.

222 TOR is a conserved serine/threonine kinase, which possesses HEAT repeats at
223 the N-terminal region, and the DUF3385, the FAT, Fkbp12-rapamycin binding (FRB),
224 kinase catalytic and FATC domains at the C-terminal region (**Fig. 3A**).To assess the
225 role of the FRB domain inside Tor kinase, the FRB domain was deleted with the
226 method of homologous recombination. Compared with the Δ*Tor1*$^{+}$/*Tor*2^{-} strain, the
227 *TOR*$^{\Delta FRB}$ single-copy deletion mutants exhibited similar defects in vegetative growth,
228 conidiation, sclerotia formation, cell wall stress and rapamycin sensitivity (**Fig.**
229 **3B,3C,S4,S5**). In *F. graminearum*, the S1866L mutation in the FgTor kinase confers
230 rapamycin resistance [21]. To investigate the function of this conserved site, the
231 *TOR*^{S1904L} mutant was constructed by homologous recombination, but site-specific
232 mutation did not impair rapamycin resistance (**Fig. 3C**). Based on these observations,
233 we speculated that the FRB domain plays critical roles in the regulation of Tor kinase
234 on fungal development and rapamycin resistance in *A. flavus*.

235 **Sch9 is involved in regulating sclerotia formation and aflatoxin biosynthesis**

236 Sch9, a Ser/Thr kinase of the AGC family, is required for TORC1 to properly
237 regulate ribosome biogenesis, translation initiation, and entry into the G_0 phase in *S.*
238 *cerevisiae,* and TORC1-dependent phosphorylation is required for Sch9 activity [49].
239 The *A. flavus* putative *Sch9* (AFLA_044350) gene encode a 706 aminoacid protein
240 with 80.31% identity to the *A. nidulans* Sch9. To investigate the function of Sch9 in *A.*
241 *flavus*, we attempted to generate Sch9 deletion mutant using a homologous

242 recombination strategy. The Δ*Sch9* strain showed normal vegetative growth and
243 conidiation similar to the WT strain (**Fig. 4B**). TLC assay and quantitative analysis
244 showed a significantly decreased aflatoxin production in Δ*Sch9* strain compared to
245 WT strain (**Fig. 4C**). These results showed that Sch9 regulates aflatoxin biosynthesis
246 in *A. flavus*.

247 **Sch9 is correlate with the HOG and TOR pathways**

248 In yeast, Sch9 is required for gene expression regulated by Sko1, which is
249 directly targeted by the Hog1 MAP kinase, and Sch9 interacts *in vitro* with both Sko1
250 and Hog1[53]. To characterize the roles of Sch9 in stress response, we examined the
251 sensitivity of Δ*Sch9* to various stresses including osmotic stress and calcium stress.
252 Compared with the WT strain, Δ*Sch9* significantly increased sensitivity to osmotic
253 stress generated by NaCl and KCl (**Fig. 4C**). In addition, the Δ*Sch9* strain was more
254 sensitive to the high concentrations of calcium stress(**Fig. S5**), these results indicated
255 that the Sch9 as a element for the calcineurin-CrzA pathway in response to calcium
256 stress. In *A. flavus*, the Sch9 kinase contain protein kinase C conserved region 2 (C2),
257 protein kinase (S_TKc), AGC-kinase C-terminal (S_TK_X) domain and a ATP
258 binding site (**Fig. 4A**). To explore the role of these domains and ATP binding site in
259 Sch9, both domains deletion strains and $Sch9^{K340A}$ mutant were constructed.
260 Compared with the Δ*Sch9* mutant, the S_TKc deletion strain ($Sch9^{\Delta S_TKc}$), S_TK_X
261 deletion strain ($Sch9^{\Delta S_TK_X}$) and $Sch9^{K340A}$ mutant exhibited similar defects in osmotic
262 stress and AFB_1 production(**Fig.4B-4D**). Therefore, we speculate that protein kinase ,
263 kinase C-terminal domain and the ATP binding site at K340 play important roles in

264 the regulation of Sch9 on osmotic and rapamycin resistance in *A. flavus*.

265 To determine if Sch9 was involved in the HOG and TOR pathways in *A. flavus*,
266 we examined the sensitivity of Δ*Sch9* to rapamycin. Compared with the WT strain,
267 the Δ*Sch9* strain was slightly more sensitive to rapamycin(**Fig. 4B**). The MAKP Hog1
268 is a element of the high osmolarity glycerol (HOG) pathway, so we further examined
269 the phosphorylation level of Hog1. Western blot analysis showed that the
270 phosphorylation level of Hog1 increased significantly in the Δ*Sch9* strain (**Fig. 4E**),
271 indicating that Sch9 influences the Hog1 in response to osmotic stress. Taken together,
272 these results reflected that Sch9 serves as a mediator of the TOR and HOG pathways
273 and regulates aflatoxin biosynthesis and multiple stress responses in *A. flavus*.

274 **TapA plays a major role in the growth, sporulation, sclerotia and aflatoxin**
275 **production**

276 Tap42, a phosphatase 2A-associating protein, is the direct target of the Tor kinase
277 in yeast. Recent results suggested that Tap42 mediates many of the Tor functions in
278 yeast, especially those involved in transcriptional modulation [55]. The *A. flavus*
279 genome has a Tap42 homolog named TapA (AFLA_092770), which predicted to
280 encode an 355 amino-acid protein shares 31.9% identity with *S. cerevisiae* Tap42. To
281 further determine the function of the TOR signaling pathway regulator TapA in *A.*
282 *flavu*s, we targeted *TapA* for gene deletion. We failed to obtain a null mutant, so we
283 generated the Δ*TapA* 1^{+}/*TapA* 2^{-} strain (containing one copy of the *TapA* gene).
284 Compared with the WT strain, the Δ*TapA* 1^{+}/*TapA* 2^{-} strain led to reduced hyphal
285 growth and conidiation (**Fig. 5A.5D**), indicating that *TapA* is important for vegetative

286 growth and conidiation. In addition, the Δ*TapA 1*$^{+}$/*TapA* 2^{-} strain was unable to
287 produce any sclerotia (**Fig. 5B**), and almost lost its capability in AFB_1 production
288 compared to the WT strain, suggesting that TapA is essential for sclerotia formation
289 and biosynthesis of AFB_1 (**Fig. 5C**). The rapamycin sensitivity test showed that the
290 Δ*TapA 1*$^{+}$/*TapA* 2^{-} strain exhibited decreased sensitivity to rapamycin (**Fig. 5A**).
291 Furthermore, the expression of *nsdC*, *nsdD* and *sclR* were significantly decreased in
292 Δ*TapA1*$^{+}$/*TapA* 2^{-} strain compared to those in the WT(**Fig. 5F**). These findings
293 revealed that the TapA plays an important positive role in growth, sporulation,
294 sclerotia and AF biosynthesis in *A. flavus*.

295 **TipA regulates growth, conidia, sclerotia and aflatoxin biosynthesis.**

296 In *S. cerevisiae*, Tip41 was identified as a Tap42-interacting protein and has been
297 measured to function as a negative regulator of Tap42, which downregulates TORC1
298 signaling via activation of PP2A phosphatase [35]. The putative Tip41 orthologue in *A.*
299 *flavus* named TipA(AFLA_047310). The amino acid sequence of TipA shares 40.49%
300 similarity to *S. cerevisiae* Tap41. To elucidate the function of TOR signaling pathway
301 protein TipA in *A. flavu*s, we generated the TipA deletion mutant. The Δ*TipA* strain
302 exhibited smaller diameter colonies on PDA compared to the WT strain, and the
303 number of conidia produced by Δ*TipA* strain was significantly reduced than that by
304 the WT strain on PDA (**Fig. 5A**). In addition, the Δ*TipA* strain was unable to produce
305 any sclerotia (**Fig. 5B**), and TLC analyses indicated that the deletion of TipA led to a
306 considerable decrease in AFB_1 production on YES (**Fig. 5C**). Meanwhile, the Δ*TipA*
307 strain exhibited decreased sensitivity to rapamycin (**Fig. 5A**). Moreover, the

308 expression levels of genes *nsdC* and *nsdD* showed a decrease in Δ*TipA* strain
309 compared to WT (**Fig. 5F**). These results indicated that TipA is important for growth,
310 conidia, sclerotial and aflatoxin biosynthesis in *A. flavus*.

311 **Phosphatase SitA and Ppg1 are involved in growth, conidiation and sclerotia**
312 **formation**

313 In *S. cerevisiae*, Tap42 also interacts with the catalytic subunits of Type 2A
314 phosphatases, such as Pph21, Pph22, Pph3, Sit4 and Ppg1, which is controlled by the
315 Tor signaling pathway [36]. Phosphatase SitA(AFLA_108450) and
316 Ppg1(AFLA_132610) were identified in *A. flavus*, which encode putative orthologs of
317 Sit4 and Ppg1 in *S. cerevisiae.* To determine the biological functions of phosphatase
318 SitA and Ppg1 in *A. flavus*, we disrupted the *SitA* and *Ppg1* by homologous
319 recombination strategy. To further study the relationship between phosphatase SitA
320 and Ppg1, we also constructed complement and double deletion mutants. The
321 vegetative development phenotype analysis showed that the Δ*SitA*, Δ*Ppg1* and
322 Δ*SitA*/Δ*Ppg1* strains grew significantly more slowly than the WT strain on PDA (**Fig.**
323 **6A**). In addition, the Δ*SitA*, Δ*Ppg1* and Δ*SitA*/Δ*Ppg1* strains formed lower number of
324 conidiophores (**Fig. 6A**). To gain further insight into the role of SitA and Ppg1 in
325 conidiation, qRT-PCR was used to determine the transcript levels of conidial
326 synthesis-related genes (*abaA* and *brlA*). The expression levels of the *abaA and brlA*
327 genes were significantly downregulated in the Δ*SitA*, Δ*Ppg1* and Δ*SitA*/Δ*Ppg1*
328 mutants compared to WT and complemented strains(**Fig. 6G**). The sclerotial
329 formation analysis results showed that the Δ*SitA*, Δ*Ppg1* and Δ*SitA*/Δ*Ppg1* mutants

330 were unable to produce any sclerotia (**Fig. 6B**).To further prove these findings, we
331 conducted qRT-PCR to determine the expression levels of three regulators (*NsdC*,
332 *NsdD* and *SclR*) of sclerotia development. Our results showed that the expression
333 levels of *NsdC*, *NsdD* and *SclR* were all downregulated in the Δ*SitA*, Δ*Ppg1* and
334 Δ*SitA*/Δ*Ppg1* mutants(**Fig. 6H**), which is consistent with the sclerotia production
335 observed in the Δ*SitA*, Δ*Ppg1* and Δ*SitA*/Δ*Ppg1*. These results showed that SitA and
336 Ppg1 are crucial for hyphal development, conidiation and sclerotia formation in *A.*
337 *flavu*s.

338 **SitA and Ppg1 play different roles in regulating aflatoxin biosynthesis**

339 Previous studies have demonstrated that protein phosphorylation is critical for the
340 regulation of AFs biosynthesis, which are the toxic and carcinogenic secondary
341 metabolites of *A. flavus* [37]. We assayed AFB_1 biosynthesis in the Δ*SitA*, Δ*Ppg1* and
342 Δ*SitA*/Δ*Ppg1* mutants, and TLC analyses indicated that Δ*SitA* and Δ*SitA*/Δ*Ppg1*
343 strains produced less AFB_1, while the level of AFB_1 produced by Δ*Ppg1* was
344 markedly increased compared to that of the WT and complemented strains (**Fig. 6C**).
345 The expression levels of aflatoxin synthesis-related genes (structural genes: *aflO*, *aflP,*
346 *aflQ* and *aflJ*, and regulatory genes: *aflR* and *aflS*) were determined by qRT-PCR in
347 the Δ*SitA*, Δ*Ppg1* and Δ*SitA*/Δ*Ppg1* mutants, and the result showed that the expression
348 levels of those genes were drastically downregulated in the Δ*SitA* and Δ*SitA*/Δ*Ppg1*
349 mutants, while upregulated in Δ*Ppg1* mutants when compared to those of the WT and
350 complemented strains(**Fig. 6I**). These results indicated that SitA and Ppg1 play
351 different roles in regulating aflatoxin biosynthesis in *A. flavu*s.

352 **SitA and Ppg1 are important for pathogenicity**

353 To investigate the pathogenicity of phosphatases SitA and Ppg1 on crops, we
354 conducted pathogenicity tests on peanut and maize. The results showed that WT and
355 complement strains resulted in full virulence on all peanut and maize seeds, while the
356 Δ*SitA*, Δ*Ppg1* and Δ*SitA*/Δ*Ppg1* mutants exhibited more flawed colonization on
357 peanut and maize seeds (**Fig. 7A**). In addition, the number of conidial productions of
358 these mutants on the infected peanut seeds also dramatically decreased compared to
359 those of WT and complement strains (**Fig. 7C**). TLC analyses indicated that the
360 Δ*Ppg1* mutant produced more AFB_1 on peanut and maize, while the level of aflatoxin
361 produced by Δ*SitA* and Δ*SitA*/Δ*Ppg1* mutants on peanut and maize were significantly
362 reduced compared to WT and complement strains (**Fig. 7B and 7D**). This is
363 consistent with the above results of aflatoxin biosynthesis of all mutants in the
364 medium. All these data showed that SitA and Ppg1 are important for crop seeds
365 pathogenicity.

366 **SitA and Ppg1 are involved in regulating cell wall integrity**

367 To explore the role of phosphatases SitA and Ppg1 in response to cell wall stress,
368 all strains were cultured on PDA amended with CFW and CR. We found that the
369 relative growth inhibition of Δ*SitA*, Δ*Ppg1* and Δ*SitA*/Δ*Ppg1* mutants induced by cell
370 wall stress were significantly increased compared to WT and complement strains (**Fig.
371 8A and 8B**). Further studies by qRT-PCR showed that expression levels of genes
372 associated with synthetic cell walls, such as chitin synthase genes *chsA*, *chsB*, *chsC*
373 and *chsD*, were significantly decreased in the Δ*SitA*, Δ*Ppg1* and Δ*SitA*/Δ*Ppg1* strains

374 (**Fig. 8C**). Western blot analysis showed that the phosphorylation level of Slt2 was
375 higher in Δ*SitA*, Δ*Ppg1* and Δ*SitA*/Δ*Ppg1* than that in the WT strain (**Fig. 8D**). To sum
376 up, the phosphatases SitA and Ppg1 maintained the integrity of the cell wall by
377 positively regulating the expression of those genes.

378 **The phosphatase complex Nem1/Spo7 are important for growth, conidiation,**
379 **aflatoxin and LD biogenesis.**

380 Lipid droplets (LDs) are spherical organelles, which appear in the cytosol of
381 some prokaryotic and most eukaryotic cells upon energy surplus. The FgTOR
382 pathway regulates the phosphorylation status of FgNem1 mainly via the
383 FgPpg1/Sit4-FgCak1/other kinase cascade in *F. graminearum* [7]. In this study, we
384 observed that rapamycin-treated hyphae led to the accumulation of LD biogenesis(**Fig.**
385 **9A**), suggesting that the TOR pathway may regulate the LD biogenesis. However, the
386 functions of LDs and the underlying regulatory mechanism of LD biosynthesis are
387 still largely unknown. In order to explore the regulatory mechanism of the TOR
388 pathway that regulates LD biogenesis in *A. flavu*s, we examined LD accumulation in
389 Δ*Sch9,* Δ*SitA* and Δ*Ppg1*. BODIPY staining assays showed that LD biogenesis was
390 not induced in the Δ*SitA* and Δ*Ppg1* strains treated with rapamycin compared to those
391 in the WT and Δ*Sch9* strains (**Fig. 9A-D**). These results indicated that LD biogenesis
392 induced by rapamycin is largely dependent on the phosphatases SitA and Ppg1 in *A.*
393 *flavu*s. In *F. graminearum,* the phosphatase FgNem1/FgSpo7 complex was involved
394 in induction of LD biogenesis by rapamycin. Phosphatase Nem1(AFLA_002649) and
395 Spo7 (AFLA_028590) were identified in *A. flavu*s, which encode putative orthologs

396 of FgNem1 and FgSpo7 in *F. graminearum.* To investigate the function of Nem1 and
397 Spo7 gene in *A. flavu*s, Δ*Nem1* and Δ*Spo7* mutants was constructed with homologous
398 recombination. The Δ*Nem1* and Δ*Spo7* mutants exhibited a significant decrease in
399 vegetative growth and conidiation compared to WT(**Fig. 10A**). TLC assay and
400 quantitative analysis showed a significantly decreased aflatoxin production in Δ*Nem1*
401 and Δ*Spo7* compared to WT(**Fig. 10B**). In addition, BODIPY staining showed no
402 visible lipid droplets in the hyphae of Δ*Nem1* and Δ*Spo7* after rapamycin
403 treatment(**Fig. 10C**). Taken together, these results indicated that Nem1/Spo7 are
404 involved in vegetative growth, conidiation, aflatoxin and LD biogenesis.

405 **Discussion**

406 Aflatoxins (AFs) are a class of toxic secondary metabolites produced by *A.*
407 *flavus*, including aflatoxin B_1, B_2, G_1 and G_2, among which AFB_1 has been regarded
408 as the most pathogenic and toxic aflatoxin [38]. Therefore, understanding the
409 regulatory mechanism of fungal secondary metabolite biosynthesis would help in
410 exploiting aflatoxin control in *A. flavu*s. In this study, we demonstrated that the target
411 of the rapamycin (TOR) signaling pathway plays critical roles in regulating growth,
412 sporulation, sclerotia and aflatoxin production in *A. flavu*s. Through functional studies
413 of nine genes in the TOR signaling pathway, we explored the conservation and
414 complexity of the TOR signaling pathway in *A. flavu*s. In addition, we constructed a
415 crosstalk network between TOR and other signaling pathways (MAPK, CWI) and
416 analyzed the specific regulatory process. We proposed that the TOR signaling

417 pathway interacts with other signaling pathways (MAPK, CWI, calcineurin-CrzA
418 pathway) to regulate the responses to various environmental stresses(**Fig. 11**). Our
419 results might provide new insights into the biological control of *A. flavus*.

420 We found that rapamycin not only affects the growth and sporulation of *A. flavu*s,
421 but also strongly inhibits sclerotia production and aflatoxin biosynthesis (**Fig. 1A-1C**).
422 This inhibitory effect has been observed in a variety of fungi, including *Candida*
423 *albicans* [39], *Cryptococcus neoformans* [39], *Podospora anserine* [40], *Aspergillus*
424 *nidulans* [26], *Magnaporthe oryzae* [8], and *Fusarium graminearum* [21], suggesting that
425 the function of the TOR signaling pathway may be conserved in filamentous fungi.
426 The number of FK506-binding proteins varies among species: there are four FKBPs
427 protein in *S. cerevisiae* and three FKBPs protein in *S. pombe* [34]. In *S. cerevisiae*,
428 rapamycin can bind to FKBP protein, irreversibly inhibit the G_1 phase of the cell cycle
429 and control cell growth [46]. The entomopathogenic fungus *Beauveria bassiana*
430 contains three putative *FKBP* genes, and disruption of *BbFKBP12* significantly
431 increases the resistance to rapamycin and FK506 [41]. The plant pathogenic fungus *F.*
432 *graminearum* harbors three FKBPs protein, among which deletion of *FgFKBP12*
433 leads to resistance to rapamycin [21]. In this study, we showed that FKBP3 is involved
434 in sclerotia and aflatoxin biosynthesis and rapamycin resistance in *A. flavu*s(**Fig.**
435 **2A-2C**), and the conserved site K19 of *FKBP3* regulated the aflatoxin biosynthesis
436 and rapamycin resistance(**Fig. 2E-2G**). Previous research has shown that FKBP12
437 was characterized as the receptor of FK506 and rapamycin, which has been the most
438 extensively documented in different fungi. The deletion of *FKBP12* confers the

439 resistance to rapamycin in *C. albicans* [39] and *C. neoformans* [39]. Similar phenotypes
440 are observed in other fungi, such as *F. graminearum*[21], *B. bassiana* [41]and *Mucor*
441 *circinelloides*[30], and the *FKBP12* mutants have significantly increased resistance to
442 rapamycin and FK506 in these filamentous fungi. In *Botrytis cinerea* [28], the deletion
443 of *BcFKBP12* cause a reduction of the virulence of strain T4, while knockout of the
444 *FKBP12* gene did not affect the pathogenic development of the strain B05.10. Thus,
445 we proposed that these FKBPs may perform similar functions in fungi.

446 The Tor kinase acts as a core element of the TOR signaling pathway, which is
447 evolutionarily conserved in fungi, plants and mammals [45]. TOR assembles into two
448 distinct multiprotein complexes: TORC1 and TORC2. A defining feature of TORC1 is
449 the interaction of TOR with KOG1 (Raptor in mammals) and its sensitivity to a
450 rapamycin-FKBP12 complex [61]. Tor kinase is widely conserved both structurally and
451 as the target of FKBP-rapamycin. Almost all other eukaryotes, including plants,
452 worms, flies, and mammals, have a single Tor gene, whereas *S. cerevisiae* has two Tor
453 genes [47]. Tor kinase is widely conserved both structurally and as the target of
454 FKBP-rapamycin, which have similar domains including HEAT-like, FAT, FRB,
455 kinase and FATC domains. The FRB domain is the binding region of the
456 FKBP-Rapamycin complex, and rapamycin resistance is caused by the disruption of
457 the FRB domain[47]. The homology comparison and phylogenetic analysis revealed
458 that there is the only Tor kinase gene predicted in *A. flavus.* To determine its function,
459 we generated the *Tor* single-copy deletion mutant by homologous recombination. We
460 found that Tor was involved in the vegetative growth and asexual development of *A.*

461 *flavus*(**Fig. 3C**). In addition, Tor responds to various stresses including osmotic and
462 oxidative stresses, cell wall-damaging agents and rapamycin(**Fig. 3F, S6**). Our results
463 revealed that Tor kinase and its FRB domain play very important roles in the
464 morphogenesis, mycotoxin biosynthesis, and multiple stress responses of *A. flavus.*
465 Previous findings demonstrated that Tor kinase could function as a molecular switch
466 connecting an iron cue to defend against pathogen infection in *C. elegans* [57]. In *A.*
467 *fumigatus*, Tor kinase represents a central regulatory node controlling genes and
468 proteins involved in nutrient sensing, stress response, cell cycle progression, protein
469 biosynthesis and degradation, as well as adaptation to low iron conditions[58]. In *F.*
470 *graminearum*, the Tor point mutation (S1866L) prevents Fkbp12-rapamycin complex
471 from binding to the FgFRB domain of FgTor [21]. We also constructed a point mutant
472 strain *TOR*^{S1904L}, but the sensitivity to rapamycin is consistent with the WT strain,
473 which may be related to the functional variances of the Tor site (S1866L) in different
474 species.

475 In *S. cerevisiae*, the protein kinase Sch9 is a major downstream effector of
476 TORC1, which plays important roles in stress resistance, longevity and nutrient
477 sensing [59]. In addition, the TORC1-Sch9 pathway acts as a crucial mediator of
478 chronological lifespan [50]. In filamentous fungi, there is a complex network of
479 interactions between TOR and HOG pathways. In *F. graminearum* [7], FgSch9 and
480 FgHog1 mutants exhibited increased sensitivity to osmotic and oxidative stresses, and
481 this defect was more severe in the FgSch9/FgHog1 double mutant. The
482 phosphorylation level of FgHog1 increased significantly in Δ*FgSch9*, and the affinity

483 capture-MS assay showed that TOR was one of the proteins co-purifying with FgSch9.
484 These results suggest that FgSch9 serves as a mediator for the TOR and HOG
485 pathways[7]. In addition, FgSch9 regulates hyphal differentiation, asexual
486 development, virulence and DON biosynthesis, which is also involved in the
487 regulation of sensitivity to rapamycin, cell wall-damaging agents, fungicide, osmotic
488 and oxidative stresses[7]. In *A. fumigatus*, the *SchA* mutant was sensitive to rapamycin,
489 high concentrations of calcium and hyperosmotic stress, and SchA was involved in
490 iron metabolism. The *SchA* mutant showed increased phosphorylation of SakA upon
491 osmotic stress[51]. In this study, we discovered that Sch9 is involved in regulating
492 aflatoxin biosynthesis (**Fig.4C**), and responses to various stresses including osmotic
493 stress, cell wall-damaging agents and rapamycin (**Fig.4B**). The S_TKc domain
494 deletion strain ($Sch9^{\Delta S_TKc}$) , S_TK_X domain deletion strain ($Sch9^{\Delta S_TK_X}$) and
495 $Sch9^{K340A}$ mutant exhibited similar phenotype with Δ*Sch9* strain(**Fig. 4C-4D**). These
496 findings revealed that Sch9 plays an important role in the biological synthesis of
497 aflatoxin and multiple stresses mainly via its kinase domain, kinase-C domain and
498 ATP binding site k340. We also found that the phosphorylation level of Hog1
499 increased significantly in the Δ*Sch9* strain(**Fig. 4E**). Based on the above results, we
500 speculated that Sch9 serves as a mediator for the complex network of interactions
501 amongst the TOR and HOG signaling pathways.

502 In *S. pombe*, Tip41 (a Tap42-interacting protein) plays an important role in the
503 cellular responses to nitrogen sources by regulating type 2A phosphatases [42]. In *S.*
504 *cerevisiae*, Tap42-phosphatase complexes associate with TORC1, and Tip41

505 downregulates TORC1 signaling via activation of PP2A phosphatase [34]. Unlike yeast
506 Tip41, TIPRL, a mammalian Tip41-like protein, has a positive effect on mTORC1
507 signaling through the interaction with PP2Ac [43]. While the interaction between Tip41
508 and Tap42 was not observed in the filamentous fungi. The Y2H assay showed that the
509 FgTip41 interacts with phosphatase FgPpg1 rather than FgTap42, while the FgTap42
510 bind with phosphatases FgPp2A, implying that FgTap42, FgPpg1 and FgTip41 form a
511 heterotrimer in *F. graminearum* [21]. FgTip41 is associated with mycotoxin production
512 and pathogenicity in *F. graminearum*, but Δ*FgTip41* had no detectable changes in
513 sensitivity to rapamycin[21]. In the rice blast fungus *M. oryzae*, MoTip41 does not
514 interact with the MoTap42, but MoTip41 can bind with phosphatase MoPpe1 to
515 mediate crosstalk between TOR and cell wall integrity signaling[9]. In this study, we
516 found that the TapA and TipA were essential for growth, conidia, sclerotia and
517 aflatoxin biosynthesis in *A. flavus*(**Fig. 5A-5C**). The *TapA* single-copy deletion
518 mutant exhibited decreased sensitivity to rapamycin. However, the TipA deletion
519 mutant had no detectable changes in sensitivity to rapamycin. These results indicated
520 that the functions of TapA and TipA in *A. flavus* were similar to its ortholog in the
521 filamentous fungi.

522 In *S. cerevisiae*, Tap42 can bind and regulate all PP2A phosphatases, including
523 Pph3, Pph21, Pph22, Sit4 and Ppg1, participating in the TOR signaling pathway in
524 response to rapamycin treatment or nutrient deprivation [35]. Sit4 plays an important
525 role in cell growth and environmental stimuli responses, such as high glucose
526 environment, high temperature and hygromycin [44]. FgSit4 and FgPpg1 are associated

527 with various cellular processes, including mycelial growth, conidiation and DON
528 biosynthesis virulence in *F. graminearum* [21]. In addition, FgSit4 and FgPpg1 are
529 involved in the regulation of various signaling pathways, such as the TOR signaling
530 pathway, CWI pathway and lipid droplets biogenesis regulation pathway [22]. In this
531 study, we found that the phosphatase SitA and Ppg1 play critical role in vegetative
532 growth, conidiation, pathogenicity, LD biogenesis, sclerotia formation and aflatoxin
533 biosynthesis in *A. flavus*(**Fig. 6A-6C**). Additionally, SitA and Ppg1 also affect cell
534 wall integrity stresses response and rapamycin sensitivity. After the deletion of the
535 *SitA* and *Ppg1* genes, the expression level of genes related to cell wall synthesis has
536 decreased significantly, resulting in damage to the cell wall and showing a higher
537 sensitivity to cell wall integrity stress. Western blotting results showed that the
538 phosphorylation level of MAPK kinase Slt2 has increased significantly in the Δ*SitA*
539 and Δ*Ppg1* strains(**Fig. 8D**), indicating that SitA and Ppg1 have a negative regulation
540 on the CWI pathway. We concluded that phosphatases SitA and Ppg1 serve as a
541 mediator for the TOR and CWI pathways in *A. flavu*s. In *M. oryzae*, MoPpe1 is the
542 homologue of *S. cerevisiae* serine/threonine protein phosphatase Sit4/Ppe1, which is
543 required for vegetative growth, conidiation and full virulence. MoPpe1 and MoSap1
544 function as an adaptor complex linking CWI and TOR signaling and the activation of
545 the TOR pathway leads to suppression of CWI signaling[8]. In addition, the
546 phosphatase MoPpe1 interacts with phosphatase-associated protein MoTip41 to
547 mediate crosstalk between TOR and CWI signaling[8]. These results suggest that
548 phosphatase ppe1 interacts with different proteins to coordinate the TOR and CWI

549 signaling pathways in regulating the growth and pathogenicity of rice blast fungus *M.*
550 *oryzae*. Taken together, we speculated that phosphatase SitA and Ppg1 may regulate
551 CWI and TOR pathways differently between species to perform their function.

552 In *F. graminearum,* the phosphatase complex FgNem1/Spo7-FgPah1 cascade
553 plays important roles in fungal development, DON production and LD biogenesis[22].
554 In this study, our results indicated that Nem1 and Spo7 are important for asexual
555 development and secondary metabolism of *A. flavus*. We also found that LD
556 biogenesis mediated by the Nem1/Spo7 and SitA/Ppg1 in *A. flavu*s. These
557 observations imply the PP2A phosphatases are core phosphatase in the LD biogenesis
558 signaling network, there should be other kinases involved in regulating the LD
559 biogenesis. It seems that phosphatases may be related to cross-talking among the TOR
560 and LD biogenesis signaling network. The exact molecular mechanism is required to
561 investigate the relationship between phosphatase and other kinase and to explore
562 regulatory mechanism and biological functions of the LDs.

563 In conclusion, we identified the complex regulatory network that elucidates how
564 crosstalk between TOR, HOG and CWI signaling modulates the development,
565 aflatoxin biosynthesis and pathogenicity of *A. flavus*. By resolving the functions of
566 genes related to the TOR signaling pathway, our findings can lay a solid foundation
567 for an in-depth understanding of the molecular mechanism of *A. flavus* pathogenicity,
568 which would provide novel insight for controlling AF contamination and reducing *A.*
569 *flavus* infection.

570

571 # Materials and methods

572 **Strains and cultural conditions**

573 The *A. flavus* strains in this study were shown in S1 Table . All strains were
574 cultured on potato dextrose agar (PDA), yeast extract-sucrose agar (YES) and yeast
575 extract-glucose agar (YGT) at 37℃ for growth and conidiation assays respectively,
576 and YES liquid medium and Potato dextrose broth (PDB) were used to detect
577 aflatoxin production at 29℃.

578 **Constructions of gene deletion and complementation mutants**

579 The gene deletion and complementation strains were constructed using the
580 SOE-PCR strategy according to previously described methods [32]. The primers used
581 to amplify the flanking sequences of each gene were listed in S2 Table. The putative
582 gene deletion mutants were verified by PCR and RT-PCR assays with the relevant
583 primers(Fig S1) and further confirmed by sequencing analysis.

584 **Growth, conidiation and sclerotia analysis**

585 To assess mycelial growth and conidia formation, 1 μL of 10^6 spores/mL conidia
586 of all strains were point inoculated onto the center of YES, PDA and YGT agar
587 medium respectively, and then cultured at 37℃ for 5 days in the dark. The colony
588 diameters were measured every day, and the conidia were washed by 0.07%
589 Tween-20 and counted using a hemocytometer and microscope[37]. For sclerotia
590 formation analysis, each strain was inoculated and grown on CM agar medium at
591 37℃ in the dark for 7 days, and then 75% ethanol was used to wash away mycelia

592 and conidia on the surface of the medium[60].The assays were repeated at least three
593 times.

594 **Extraction and quantitative analysis of aflatoxin**

595 To extract AF and quantify the AF production, 1 μL of 10^6 spores/mL conidia of
596 all strains were point inoculated onto liquid YES or PDB medium and cultures were
597 incubated at 29°C in the dark for 6 days. AF were extracted from the media and
598 detected by thin layer chromatography (TLC)[60].In addition, the standard AFB_1 was
599 used for visual comparison, and AF was quantitative analyzed by the Image J tool.
600 The assays were repeated at least three times.

601 **Stress assay**

602 To determine the roles of the gene in *A. flavus* responsing to various
603 environmental stresses, 1 μL of 10^6 spores/mL conidia of all strains were point
604 inoculated onto these PDA solid plates supplemented with different agents, including
605 1M NaCl,1M KCl and 1M $CaCl_2$ treatment for osmotic stress, 100μg/mL SDS, 200
606 μg/mL Calcofluor white (CFW) and 200 μg/mL Congo red (CR) treatment for cell
607 wall stress. After 5 days of incubation at 37°C in the dark, the relative inhibition rates
608 were calculated[37]. The assays were repeated at least three times.

609 **Seeds infection assays**

610 To measure the pathogenicity of *A. flavus*, all peanut and maize seeds were
611 washed in 0.05% sodium hypochlorite, 75% ethanol and sterile water respectively,
612 and then all peanut and maize seeds were soaked in sterile water supplemented with

613 10^6 spores/mL of all strains at 29°C in the dark for 60 min. After the conidia adhesion,
614 the seeds were cultured at 29°C for 6 days in the dark[60].

615 **Quantitative RT-PCR**

616 For real-time quantitative PCR (qPCR) assays, the *A. flavus* strains were cultured
617 in PDA medium at 29°C for 3 days in the dark. Total RNA was extracted from the
618 mycelia of all strains, and cDNA was synthesized with First Strand cDNA Synthesis
619 Kit, and then the cDNA was used as the template for qRT-PCR analysis with SYBR
620 Green qPCR mix. The relative transcript level of each gene was calculated by the
621 $2^{-\Delta\Delta CT}$method[62].

622 **Western blot analysis**

623 To extract the total protein, the mycelia of each strain were cultured in YES
624 liquid medium for 48 h, then the sample was grinded under liquid nitrogen to a fine
625 powder and transfered to a 1.5 mL microcentrifuge tube added with RIPA lysis buffer
626 and 1 mM PMSF protease inhibitor. Proteins were separated by 12% SDS-PAGE and
627 transferred onto a polyvinylidene fluoride (PVDF) membrane. Phosphorylation levels
628 of Hog1 and Slt2 were detected by Phospho-p38 MAPK antibody (Cell Signaling
629 Technology, Boston, MA, USA) and Phospho-p44/42 MAPK (Erk 1/2) antibody (Cell
630 signaling Technology, MA, USA), respectively[60]. The experiment was conducted
631 three times independently.

632 **Statistical analysis**

633 All data were measured with means ± standard deviation (SD) of three biological
634 replicates. Graph Pad Prism 7 software was used for statistical and significance

635 analysis, and p-values < 0.05 was represented statistical significance. Student's *t*-test
636 was used to compare the two means for differences, whereas Tukey's multiple
637 comparisons were used for testing multiple comparisons.
638

639 Acknowledgments

640 The authors also thank Professor Zhenhong Zhuang, Jun Yuan, Yu Wang, Kunzhi
641 Jia, Xiuna Wang and Xinyi Nie for their help in the experiments. This work was
642 supported by the National Natural Science Foundation of China (Grant No.
643 31972214).

644 Author contributions

645 Guoqi Li and Xiaohong Cao designed the experiments. Guoqi Li, Xiaohong Cao
646 and Qianhua Zeng performed the experiments. Guoqi Li, Xiaohong Cao and Shihua
647 Wang analyzed the data. Guoqi Li, Elisabeth Tumukunde and Shihua Wang wrote the
648 manuscript. The manuscript was discussed and revised by all the authors.

649 References

650 [1] Klich MA. *Aspergillus flavus*: the major producer of aflatoxin. Mol Plant Pathol.
651 2007; 8(6): 713-22.
652 [2] Hedayati MT, Pasqualotto AC, Warn PA, et al. *Aspergillus flavus*: human
653 pathogen, allergen and mycotoxin producer. Microbiology (Reading). 2007;
654 153(Pt 6): 1677-1692.
655 [3] Khan R, Ghazali FM, Mahyudin NA, et al. Biocontrol of aflatoxins using

656 non-aflatoxigenic *Aspergillus flavus*: a literature review. J Fungi (Basel). 2021;
657 7(5): 381.
658 [4] Yabe K, Nakajima H. Enzyme reactions and genes in aflatoxin biosynthesis. Appl
659 Microbiol Biotechnol. 2004; 64(6): 745-55.
660 [5] Wullschleger S, Loewith R, Hall MN. TOR signaling in growth and metabolism.
661 Cell. 2006; 124(3): 471-84.
662 [6] Petersen J. TOR signalling regulates mitotic commitment through stress-activated
663 MAPK and Polo kinase in response to nutrient stress. Biochem Soc Trans. 2009;
664 37(Pt 1): 273-7.
665 [7] Gu Q, Zhang C, Yu F, et al. Protein kinase FgSch9 serves as a mediator of the
666 target of rapamycin and high osmolarity glycerol pathways and regulates multiple
667 stress responses and secondary metabolism in *Fusarium graminearum*. Environ
668 Microbiol. 2015; 17(8): 2661-76.
669 [8] Qian B, Liu X, Jia J, et al. MoPpe1 partners with MoSap1 to mediate TOR and
670 cell wall integrity signalling in growth and pathogenicity of the rice blast fungus
671 *Magnaporthe oryzae*. Environ Microbiol. 2018; 20(11): 3964-3979.
672 [9] Qian B, Liu X, Ye Z, et al. Phosphatase-associated protein MoTip41 interacts
673 with the phosphatase MoPpe1 to mediate crosstalk between TOR and cell wall
674 integrity signalling during infection by the rice blast fungus *Magnaporthe oryzae*.
675 Environ Microbiol. 2021; 23(2): 791-809.
676 [10] Heitman J, Movva NR, Hall MN. Targets for cell cycle arrest by the
677 immunosuppressant rapamycin in yeast. Science. 1991; 253(5022): 905-9.

678 [11] Loewith R, Jacinto E, Wullschleger S, et al. Two TOR complexes, only one of
679 which is rapamycin sensitive, have distinct roles in cell growth control. Mol Cell.
680 2002; 10(3): 457-68.
681 [12] Kim DH, Sarbassov DD, Ali SM, et al. mTOR interacts with raptor to form a
682 nutrient-sensitive complex that signals to the cell growth machinery. Cell. 2002;
683 110(2): 163-75.
684 [13] Fu L, Liu Y, Qin G, et al. The TOR-EIN2 axis mediates nuclear signalling to
685 modulate plant growth. Nature. 2021; 591(7849): 288-292.
686 [14] Bastidas RJ, Reedy JL, Morales-Johansson H, et al. Signaling cascades as drug
687 targets in model and pathogenic fungi. Curr Opin Investig Drugs. 2008; 9(8):
688 856-64.
689 [15] Rohde JR, Bastidas R, Puria R, et al. Nutritional control via Tor signaling in
690 *Saccharomyces cerevisiae*. Curr Opin Microbiol. 2008; 11(2): 153-60.
691 [16] Ishiguro J, Shibahara K, Ueda Y, et al. Fission yeast TOR signaling is essential
692 for the down-regulation of a hyperactivated stress-response MAP kinase under
693 salt stress. Mol Genet Genomics. 2013; 288(1-2): 63-75.
694 [17] Otsubo Y, Yamamato M. TOR signaling in fission yeast. Crit Rev Biochem Mol
695 Biol. 2008; 43(4): 277-83.
696 [18] Wang H, Wang X, Jiang Y. Interaction with Tap42 is required for the essential
697 function of Sit4 and type 2A phosphatases. Mol Biol Cell. 2003; 14(11): 4342-51.
698 [19] Yan G, Shen X, Jiang Y. Rapamycin activates Tap42-associated phosphatases by
699 abrogating their association with Tor complex 1. EMBO J. 2006; 25(15):

700 3546-55.

701 [20] Urban J, Soulard A, Huber A, et al. Sch9 is a major target of TORC1 in
702 *Saccharomyces cerevisiae*. Mol Cell. 2007; 26(5): 663-74.

703 [21] Yu F, Gu Q, Yun Y, et al. The TOR signaling pathway regulates vegetative
704 development and virulence in *Fusarium graminearum*. New Phytol. 2014; 203(1):
705 219-32.

706 [22] Liu N, Yun Y, Yin Y, et al. Lipid droplet biogenesis regulated by the
707 FgNem1/Spo7-FgPah1 phosphatase cascade plays critical roles in fungal
708 development and virulence in *Fusarium graminearum*. New Phytol. 2019; 223(1):
709 412-429.

710 [23] Sun G, Elowsky C, Li G, et al. TOR-autophagy branch signaling via Imp1
711 dictates plant-microbe biotrophic interface longevity. PLoS Genet. 2018; 14(11):
712 e1007814.

713 [24] Nguyen DV, Roret T, Fernandez-Gonzalez A, et al. Target of rapamycin pathway
714 in the white-rot fungus *Phanerochaete chrysosporium*. PLoS One. 2020; 15(2):
715 e0224776.

716 [25] Dementhon K, Paoletti M, Pinan-Lucarré B, et al. Rapamycin mimics the
717 incompatibility reaction in the fungus *Podospora anserina*. Eukaryot Cell. 2003;
718 2(2): 238-46.

719 [26] Fitzgibbon GJ, Morozov IY, Jones MG, et al. Genetic analysis of the TOR
720 pathway in *Aspergillus nidulans*. Eukaryot Cell. 2005; 4(9): 1595-8.

721 [27] Teichert S, Wottawa M, Schönig B, et al. Role of the *Fusarium fujikuroi* TOR

722 kinase in nitrogen regulation and secondary metabolism. Eukaryot Cell. 2006;
723 5(10): 1807-19.
724 [28] Meléndez HG, Billon-Grand G, Fèvre M, et al. Role of the *Botrytis cinerea*
725 FKBP12 ortholog in pathogenic development and in sulfur regulation. Fungal
726 Genet Biol. 2009; 46(4): 308-20.
727 [29] López-Berges MS, Rispail N, Prados-Rosales RC, et al. A nitrogen response
728 pathway regulates virulence functions in *Fusarium oxysporum* via the protein
729 kinase TOR and the bZIP protein MeaB. Plant Cell. 2010; 22(7): 2459-75.
730 [30] Bastidas RJ, Shertz CA, Lee SC, et al. Rapamycin exerts antifungal activity *in*
731 *vitro* and *in vivo* against *Mucor circinelloides* via FKBP12-dependent inhibition
732 of Tor. Eukaryot Cell. 2012; 11(3): 270-81.
733 [31] Shertz CA, Bastidas RJ, Li W, et al. Conservation, duplication, and loss of the Tor
734 signaling pathway in the fungal kingdom. BMC Genomics. 2010; 11: 510.
735 [32] Tan L, Chen H, Yu S, et al. A SOE-PCR method of introducing multiple
736 mutations into Mycoplasma gallisepticum neuraminidase. J Microbiol Methods.
737 2013; 94(2): 117-120.
738 [33] Tong M, Jiang Y. FK506-Binding Proteins and Their Diverse Functions. Curr Mol
739 Pharmacol. 2015; 9(1): 48-65.
740 [34] Galat A. Functional diversity and pharmacological profiles of the FKBPs and
741 their complexes with small natural ligands. Cell Mol Life Sci. 2013; 70(18):
742 3243-75.
743 [35] Jacinto E, Guo B, Arndt KT, et al. TIP41 interacts with TAP42 and negatively

744 regulates the TOR signaling pathway. Mol Cell. 2001; 8(5): 1017-26.

745 [36] Wang H, Wang X, Jiang Y. Interaction with Tap42 is required for the essential
746 function of Sit4 and type 2A phosphatases. Mol Biol Cell. 2003; 14(11): 4342-51.

747 [37] Ren S, Yang M, Li Y, et al. Global phosphoproteomic analysis reveals the
748 involvement of phosphorylation in aflatoxins biosynthesis in the pathogenic
749 fungus *Aspergillus flavu*s. Sci Rep. 2016; 6: 34078.

750 [38] Gizachew D, Chang CH, Szonyi B, et al. Aflatoxin B1 (AFB_1) production by
751 *Aspergillus flavus* and *Aspergillus parasiticus* on ground Nyjer seeds: The effect
752 of water activity and temperature. Int J Food Microbiol. 2019; 296: 8-13.

753 [39] Cruz MC, Goldstein AL, Blankenship J, et al. Rapamycin and less
754 immunosuppressive analogs are toxic to *Candida albicans* and *Cryptococcus*
755 *neoformans* via FKBP12-dependent inhibition of TOR. Antimicrob Agents
756 Chemother. 2001; 45(11): 3162-70.

757 [40] Dementhon K, Paoletti M, Pinan-Lucarré B, et al. Rapamycin mimics the
758 incompatibility reaction in the fungus *Podospora anserina*. Eukaryot Cell. 2003;
759 2(2): 238-46.

760 [41] Li Y, Ren H, Zhao Y, et al. Characterization of three FK506-binding proteins in
761 the entomopathogenic fungus *Beauveria bassiana*. J Invertebr Pathol. 2020; 171:
762 107334.

763 [42] Fenyvuesvolgyi C, Elder RT, Benko Z, et al. Fission yeast homologue of
764 Tip41-like proteins regulates type 2A phosphatases and responses to nitrogen
765 sources. Biochim Biophys Acta. 2005; 1746(2): 155-62.

766 [43] Nakashima A, Tanimura-Ito K, Oshiro N, et al. A positive role of mammalian
767 Tip41-like protein, TIPRL, in the amino-acid dependent mTORC1-signaling
768 pathway through interaction with PP2A. FEBS Lett. 2013; 587(18): 2924-9.
769 [44] Yoshikawa K, Tanaka T, Ida Y, et al. Comprehensive phenotypic analysis of
770 single-gene deletion and overexpression strains of *Saccharomyces cerevisiae*.
771 Yeast. 2011; 28(5): 349-61.
772 [45] Xiong Y, Sheen J. The role of target of rapamycin signaling networks in plant
773 growth and metabolism. Plant Physiol. 2014; 164(2): 499-512.
774 [46] Heitman J, Movva NR, Hiestand PC, et al. FK506-binding protein proline
775 rotamase is a target for the immunosuppressive agent FK 506 in *Saccharomyces*
776 *cerevisiae*. Proc Natl Acad Sci U S A. 1991; 88(5): 1948-52.
777 [47] Loewith R, Hall MN. Target of rapamycin (TOR) in nutrient signaling and
778 growth control. Genetics. 2011; 189(4): 1177-201.
779 [48] Kira S, Kumano Y, Ukai H, et al. Dynamic relocation of the
780 TORC1-Gtr1/2-Ego1/2/3 complex is regulated by Gtr1 and Gtr2. Mol Biol Cell.
781 2016; 27(2): 382-96.
782 [49] Urban J, Soulard A, Huber A, et al. Sch9 is a major target of TORC1 in
783 *Saccharomyces cerevisiae*. Mol Cell. 2007; 26(5): 663-74.
784 [50] Deprez MA, Eskes E, Winderickx J, et al. The TORC1-Sch9 pathway as a crucial
785 mediator of chronological lifespan in the yeast *Saccharomyces cerevisiae*. FEMS
786 Yeast Res. 2018; 18(5).
787 [51] Alves de Castro P, Dos Reis TF, et al. The *Aspergillus fumigatus* SchA^{SCH9} kinase

788 modulates SakA^{HOG1} MAP kinase activity and it is essential for virulence. Mol
789 Microbiol. 2016; 102(4): 642-671.
790 [52] Baldin C, Valiante V, Krüger T, et al. Comparative proteomics of a tor inducible
791 *Aspergillus fumigatus* mutant reveals involvement of the Tor kinase in iron
792 regulation. Proteomics. 2015; 15(13): 2230-43.
793 [53] Pascual-Ahuir A, Proft M. The Sch9 kinase is a chromatin-associated
794 transcriptional activator of osmostress-responsive genes. EMBO J. 2007; 26(13):
795 3098-108.
796 [54] Chen D, Wang Y, Zhou X, et al. The Sch9 kinase regulates conidium size, stress
797 responses, and pathogenesis in *Fusarium graminearum*. PLoS One. 2014; 9(8):
798 e105811.
799 [55] Düvel K, Broach JR. The role of phosphatases in TOR signaling in yeast. Curr
800 Top Microbiol Immunol. 2004; 279: 19-38.
801 [56] Wang H, Wang X, Jiang Y. Interaction with Tap42 is required for the essential
802 function of Sit4 and type 2A phosphatases. Mol Biol Cell. 2003; 14(11): 4342-51.
803 [57] Ma YC, Dai LL, Qiu BB, et al. TOR functions as a molecular switch connecting
804 an iron cue with host innate defense against bacterial infection. PLoS Genet. 2021;
805 17(3): e1009383.
806 [58] Baldin C, Valiante V, Krüger T, et al. Comparative proteomics of a tor inducible
807 *Aspergillus fumigatus* mutant reveals involvement of the Tor kinase in iron
808 regulation. Proteomics. 2015; 15(13): 2230-43.
809 [59] Pascual-Ahuir A, Proft M. The Sch9 kinase is a chromatin-associated

810 transcriptional activator of osmostress-responsive genes. EMBO J. 2007; 26(13):
811 3098-108.
812 [60] Ren S, Yang M, Yue Y, et al. Lysine Succinylation Contributes to Aflatoxin
813 Production and Pathogenicity in *Aspergillus flavus*. Mol Cell Proteomics. 2018;
814 17(3): 457-471.
815 [61] Adami A, García-Alvarez B, Arias-Palomo E, et al. Structure of TOR and its
816 complex with KOG1. Mol Cell. 2007; 27(3): 509-16.
817 [62] Livak KJ, Schmittgen TD. Analysis of relative gene expression data using
818 real-time quantitative PCR and the $2^{-\Delta\Delta CT}$ method. Methods.2001; 25(4):402–408

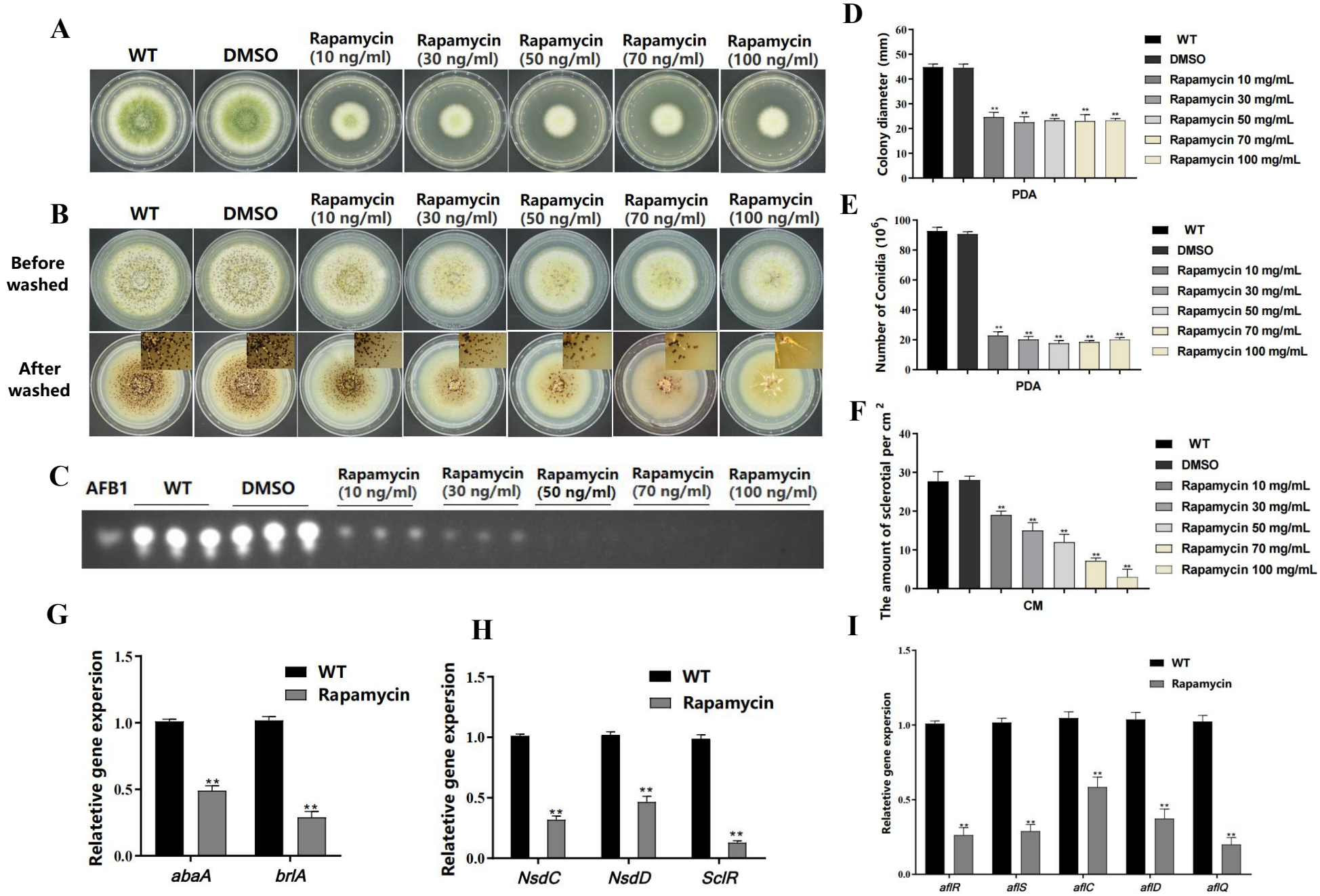
A
WT
DMSO
Rapamycin (10 ng/ml)
Rapamycin (30 ng/ml)
Rapamycin (50 ng/ml)
Rapamycin (70 ng/ml)
Rapamycin (100 ng/ml)
B
Before washed
After washed
C
AFB1
D
Colony diameter (mm)
PDA
Rapamycin 10 mg/mL
Rapamycin 30 mg/mL
Rapamycin 50 mg/mL
Rapamycin 70 mg/mL
Rapamycin 100 mg/mL
E
Number of Conidia (10^6)
F
The amount of sclerotial per cm^2
CM
G
Relatetive gene expersion
Rapamycin
abaA
brlA
H
NsdC
NsdD
SclR
I
aflR
aflS
aflC
aflD
aflQ

Fig. 1 Impacts of rapamycin on growth, sporulation , sclerotia and aflatoxin production of *Aspergillus flavus*.

(A) The *A. flavus* wild-type (WT) strain was incubated on PDA amended with different concentrations of rapamycin at 37 °C for 5 days .

(B) Colony phenotype of WT strain grown on CM medium amended with different concentrations of rapamycin at 37 °C for 7 days.

(C) TLC assay of AFB_1 production by WT strain cultured in YES liquid media at 29°C for 6 days.

(D) Statistical analysis of the diameter by the WT strain treated with different concentrations of rapamycin described in (A).

(E) Conidial quantification of the WT strain treated with different concentrations of rapamycinas as mentioned in (A).

(F) Quantitative analysis of sclerotium formation by the WT strain treated with different concentrations of rapamycin described in (C).

(G) Relative transcript levels of conidia-related genes in WT strain treated with 100 ng/mL rapamycin cultured for 48 h.

(H) Relative transcript levels of sclerotia-related genes in WT strain treated with 100 ng/mL rapamycin cultured for 48 h.

(I) Relative transcript levels of aflatoxin biosynthesis regulatory and structural genes in WT strain treated with 100 ng/mL rapamycin cultured for 48 h.

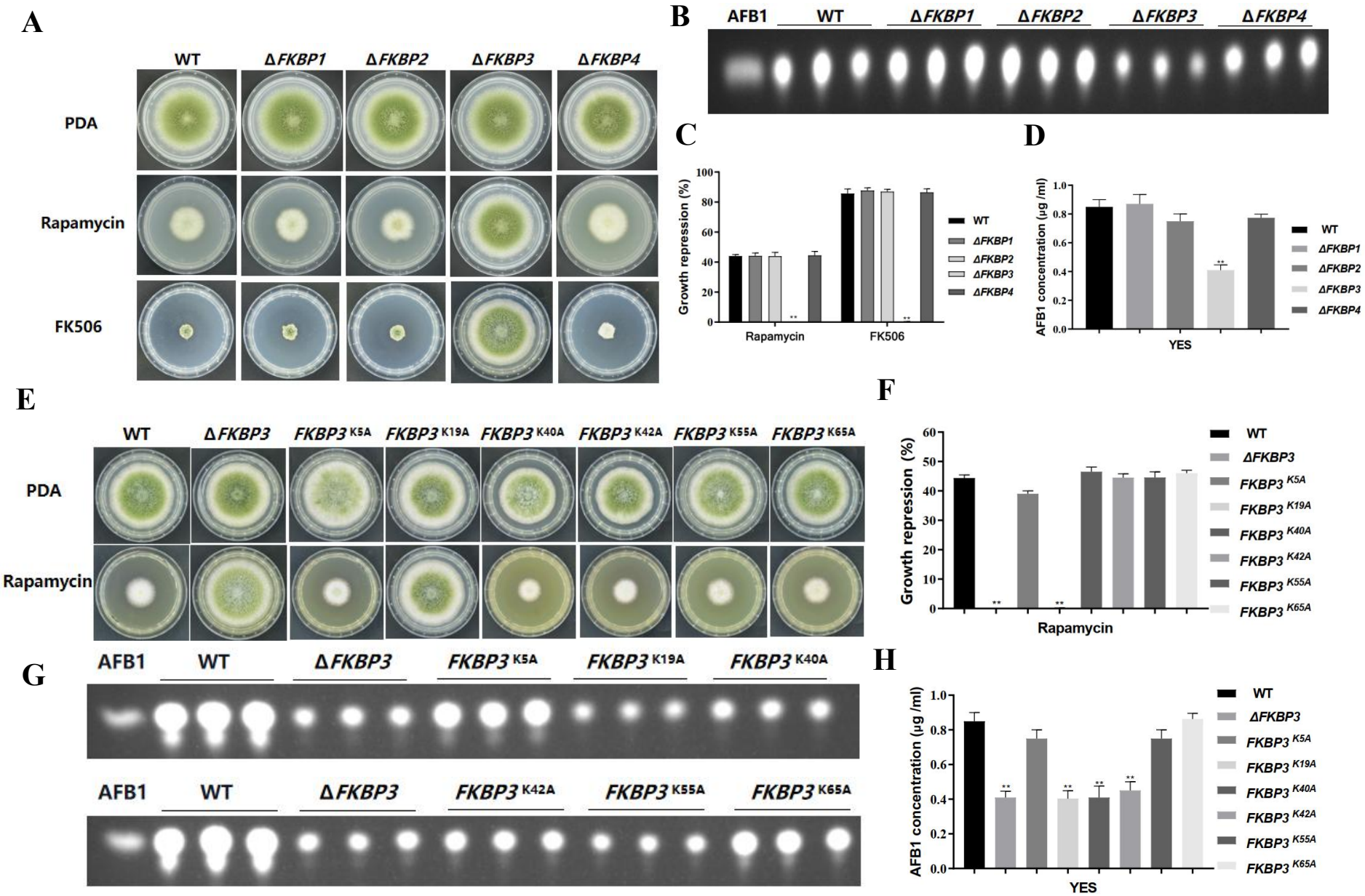
A
WT
ΔFKBP1
ΔFKBP2
ΔFKBP3
ΔFKBP4
PDA
Rapamycin
FK506
B
AFB1
WT
ΔFKBP1
ΔFKBP2
ΔFKBP3
ΔFKBP4
C
Growth repression (%)
Rapamycin
FK506
WT
ΔFKBP1
ΔFKBP2
ΔFKBP3
ΔFKBP4
D
AFB1 concentration (μg /ml)
YES
E
WT
ΔFKBP3
FKBP3 K5A
FKBP3 K19A
FKBP3 K40A
FKBP3 K42A
FKBP3 K55A
FKBP3 K65A
PDA
Rapamycin
F
Growth repression (%)
Rapamycin
G
AFB1
H
AFB1 concentration (μg /ml)
YES

Fig. 2 Disruption of FKBP3 significantly increases the resistance of *A. flavus* to rapamycin and FK506.

(A) Phenotype of *A. flavus* WT and all mutant strains (Δ*FKBP1,* Δ*FKBP2*, Δ*FKBP3* and Δ*FKBP4*) grown on PDA amended with 100 ng/mL rapamycin at 37°C for 5 days.

(B) TLC assay of AFB_1 production by the WT and all mutant strains (Δ*FKBP1,* Δ*FKBP2*, Δ*FKBP3* and Δ*FKBP4*) cultured in YES liquid medium at 29°C for 6 days.

(C) The growth inhibition rate of the WT and all mutant strains (Δ*FKBP1,* Δ*FKBP2*, Δ*FKBP3* and Δ*FKBP4*) under rapamycin stress.

(D) AFB_1 quantitative analysis of the WT and all mutant strains (Δ*FKBP1,* Δ*FKBP2*, Δ*FKBP3* and Δ*FKBP4*) described in (B).

(E) Phenotype of WT and all mutant strains (Δ*FKBP3,* K5A, K19A, K40A, K42A, K55A and K65A) grown on PDA amended with 100 ng/mL rapamycin at 37°C for 5 days.

(F) The growth inhibition rate of WT and all mutant strains (Δ*FKBP3,* K5A, K19A, K40A, K42A, K55A and K65A) under rapamycin stress.

(G) TLC assay of AFB_1 production by the WT and all mutant strains (Δ*FKBP3,* K5A, K19A, K40A, K42A, K55A and K65A) cultured in YES liquid medium at 29°C for 6 days.

(H) Relative quantification of AFB1 production in WT and all mutant strains (Δ*FKBP3,* K5A, K19A, K40A, K42A, K55A and K65A) as mentioned in (G).

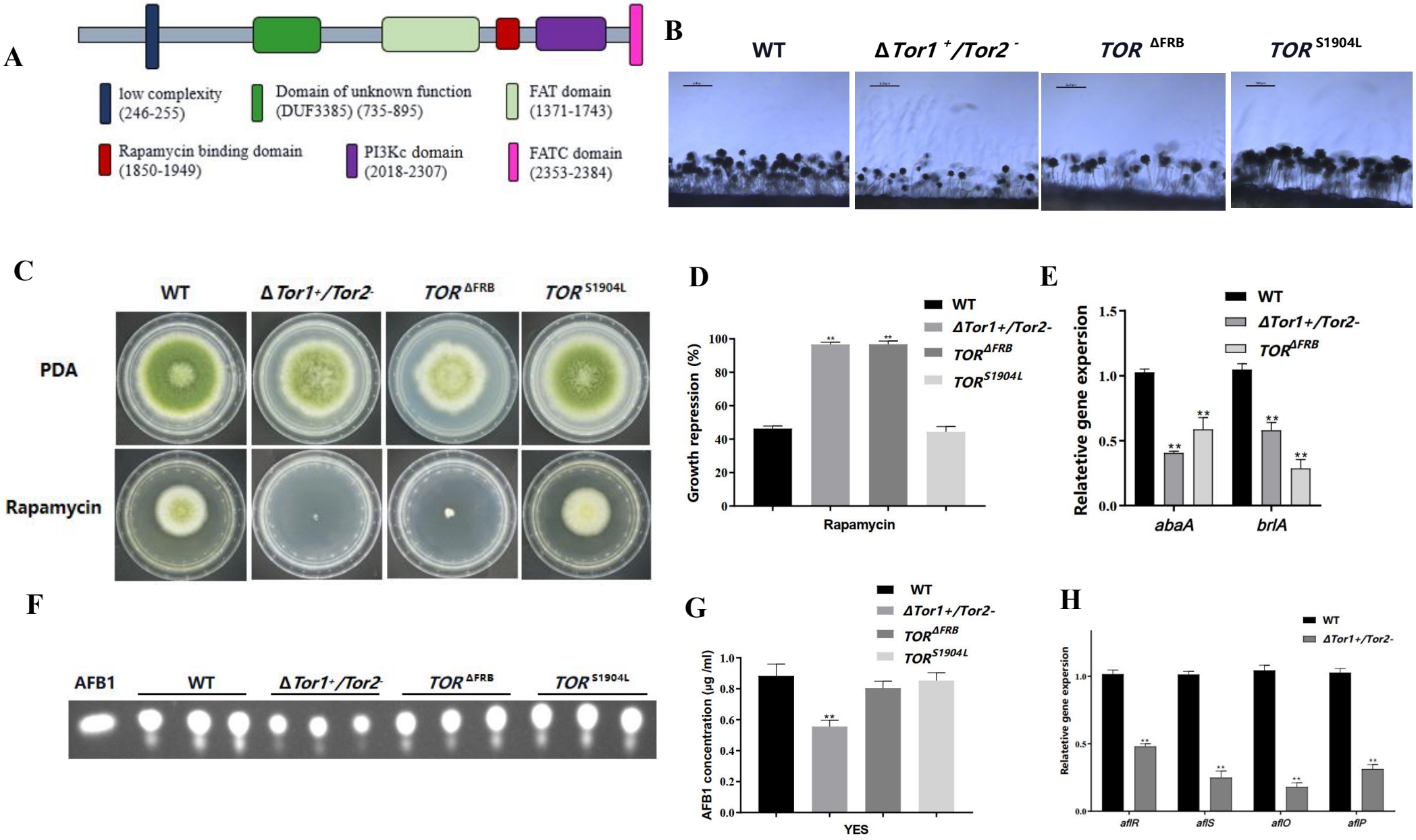
A
low complexity (246-255)
Domain of unknown function (DUF3385) (735-895)
FAT domain (1371-1743)
Rapamycin binding domain (1850-1949)
PI3Kc domain (2018-2307)
FATC domain (2353-2384)
B
WT
ΔTor1+/Tor2-
TOR ΔFRB
TOR S1904L
C
WT
ΔTor1+/Tor2-
TOR ΔFRB
TOR S1904L
PDA
Rapamycin
D
WT
ΔTor1+/Tor2-
TOR ΔFRB
TOR S1904L
Growth repression (%)
Rapamycin
E
WT
ΔTor1+/Tor2-
TOR ΔFRB
Relatetive gene expersion
abaA
brlA
F
AFB1
WT
ΔTor1+/Tor2-
TOR ΔFRB
TOR S1904L
G
WT
ΔTor1+/Tor2-
TOR ΔFRB
TOR S1904L
AFB1 concentration (μg /ml)
YES
H
WT
ΔTor1+/Tor2-
Relatetive gene expersion
aflR
aflS
aflO
aflP

Fig. 3 Tor kinase plays important roles in *A. flavus*.

(A) The structure diagram of Tor kinase.

(B) Morphology of conidiophores of *A. flavus* WT, Δ*Tor1*$^{+}$/*Tor*2^{-} , *TOR*$^{\Delta FRB}$ and *TOR*^{S1904L} strains grown on PDA medium at 37°C for 5 days as observed by microscope.

(C) Phenotype of WT, Δ*Tor1*$^{+}$/*Tor*2^{-}, *TOR*$^{\Delta FRB}$ and *TOR*^{S1904L} strains grown on PDA amended with 100 ng/mL rapamycin at 37°C for 5 days.

(D) The growth inhibition rate of WT, Δ*Tor1*$^{+}$/*Tor*2^{-}, *TOR*$^{\Delta FRB}$ and *TOR*^{S1904L} strains under rapamycin stress.

(E) Relative transcript levels of conidia-related genes in WT, Δ*Tor1*$^{+}$/*Tor*2^{-} , *TOR*$^{\Delta FRB}$ strains.

(F) TLC assay of AFB_1 production by the WT, Δ*Tor1*$^{+}$/*Tor*2^{-}, *TOR*$^{\Delta FRB}$ and *TOR*^{S1904L} strains cultured in YES liquid medium at 29°C for 6 days.

(G) Quantification analysis of AFB_1 as in (F).

(H) Relative transcript levels of aflatoxin biosynthesis regulatory and structural genes in WT and Δ*Tor1*$^{+}$/*Tor*2^{-}strains.

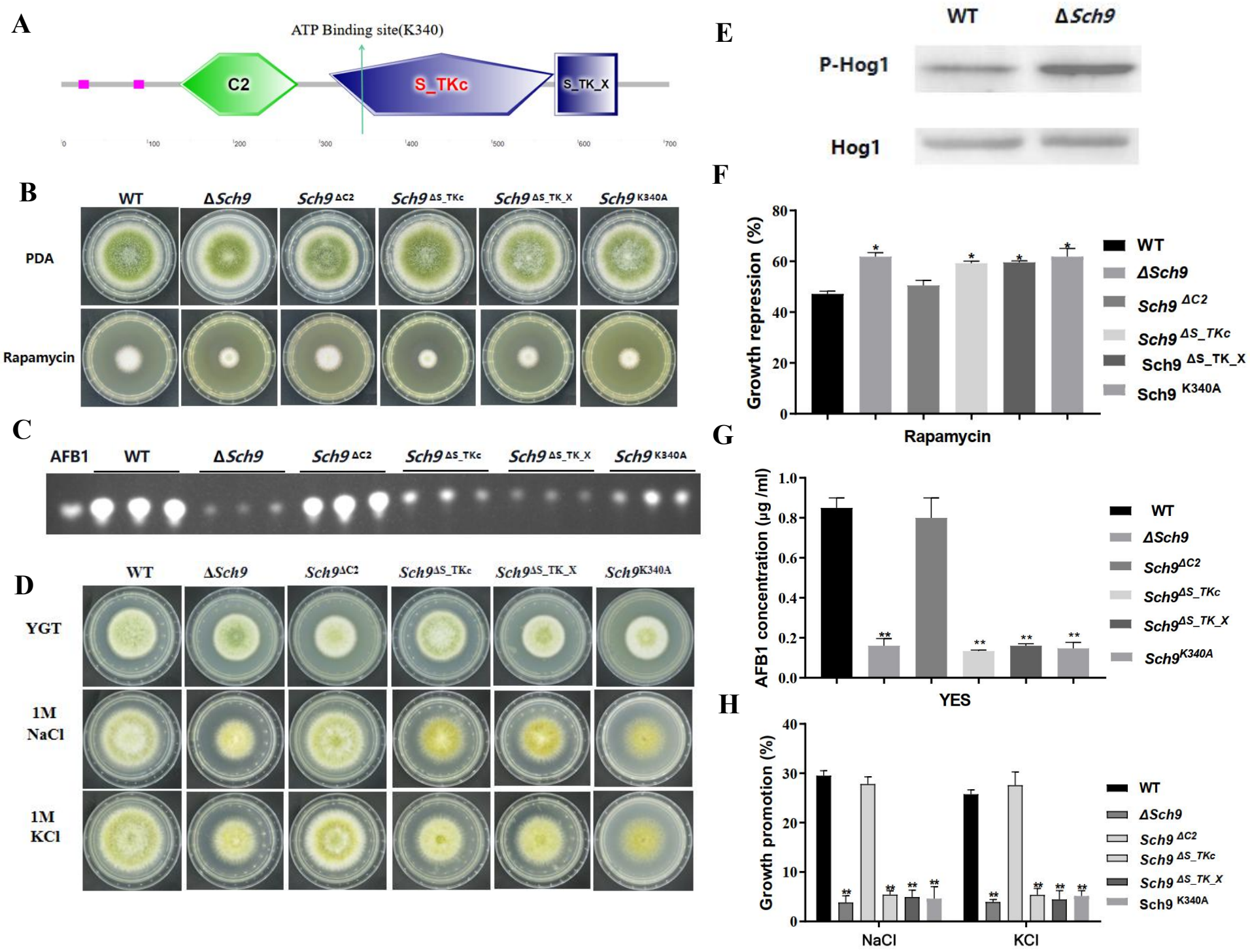
A
ATP Binding site(K340)
C2
S_TKc
S_TK_X
0
100
200
300
400
500
600
700
B
WT
ΔSch9
Sch9 ΔC2
Sch9 ΔS_TKc
Sch9 ΔS_TK_X
Sch9 K340A
PDA
Rapamycin
C
AFB1
WT
ΔSch9
Sch9 ΔC2
Sch9 ΔS_TKc
Sch9 ΔS_TK_X
Sch9 K340A
D
WT
ΔSch9
Sch9ΔC2
Sch9ΔS_TKc
Sch9ΔS_TK_X
Sch9K340A
YGT
1M NaCl
1M KCl
E
WT
ΔSch9
P-Hog1
Hog1
F
Growth repression (%)
80
60
40
20
0
Rapamycin
WT
ΔSch9
Sch9 ΔC2
Sch9 ΔS_TKc
Sch9 ΔS_TK_X
Sch9 K340A
G
AFB1 concentration (μg /ml)
1.0
0.8
0.6
0.4
0.2
0.0
YES
WT
ΔSch9
Sch9ΔC2
Sch9ΔS_TKc
Sch9ΔS_TK_X
Sch9K340A
H
Growth promotion (%)
40
30
20
10
0
NaCl
KCl
WT
ΔSch9
Sch9 ΔC2
Sch9 ΔS_TKc
Sch9 ΔS_TK_X
Sch9 K340A

Fig. 4 Sch9 is correlated with the HOG and TOR pathways.

(A) The structure diagram of Sch9 kinase.

(B) Phenotype of *A. flavus* WT, Δ*Sch9*, *Sch9*$^{\Delta C2}$, *Sch9*$^{\Delta S_TKc}$, *Sch9*$^{\Delta S_TK_X}$ and Sch9^{K340A} strains grown on PDA amended with 100 ng/mL rapamycin at 37°C for 5 days.

(C) TLC assay of AFB_1 production by the WT, Δ*Sch9*, *Sch9*$^{\Delta C2}$, *Sch9*$^{\Delta S_TKc}$,*Sch9*$^{\Delta S_TK_X}$and Sch9^{K340A} strains cultured in YES liquid medium at 29°C for 6 days.

(D) Colonies of WT, Δ*Sch9*, *Sch9*$^{\Delta C2}$, *Sch9*$^{\Delta S_TKc}$,*Sch9*$^{\Delta S_TK_X}$and Sch9^{K340A} strains on PDA media amended with 1 M NaCl and 1 M KCl for 3 days.

(E) The expressed levels of phospho-Hog1 were detected in WT and Δ*Sch9* strains.

(F) The growth inhibition rate of WT, Δ*Sch9*, *Sch9*$^{\Delta C2}$, *Sch9*$^{\Delta S_TKc}$, *Sch9*$^{\Delta S_TK_X}$ and Sch9^{K340A} strains under rapamycin stress.

(G) Quantitative analysis of AFB_1, as shown in (C).

(H) The growth promotion rate of WT, Δ*Sch9*, S*ch9*$^{\Delta C2}$, *Sch9*$^{\Delta S_TKc}$, *Sch9*$^{\Delta S_TK_X}$ and Sch9^{K340A} strains under osmotic stress.

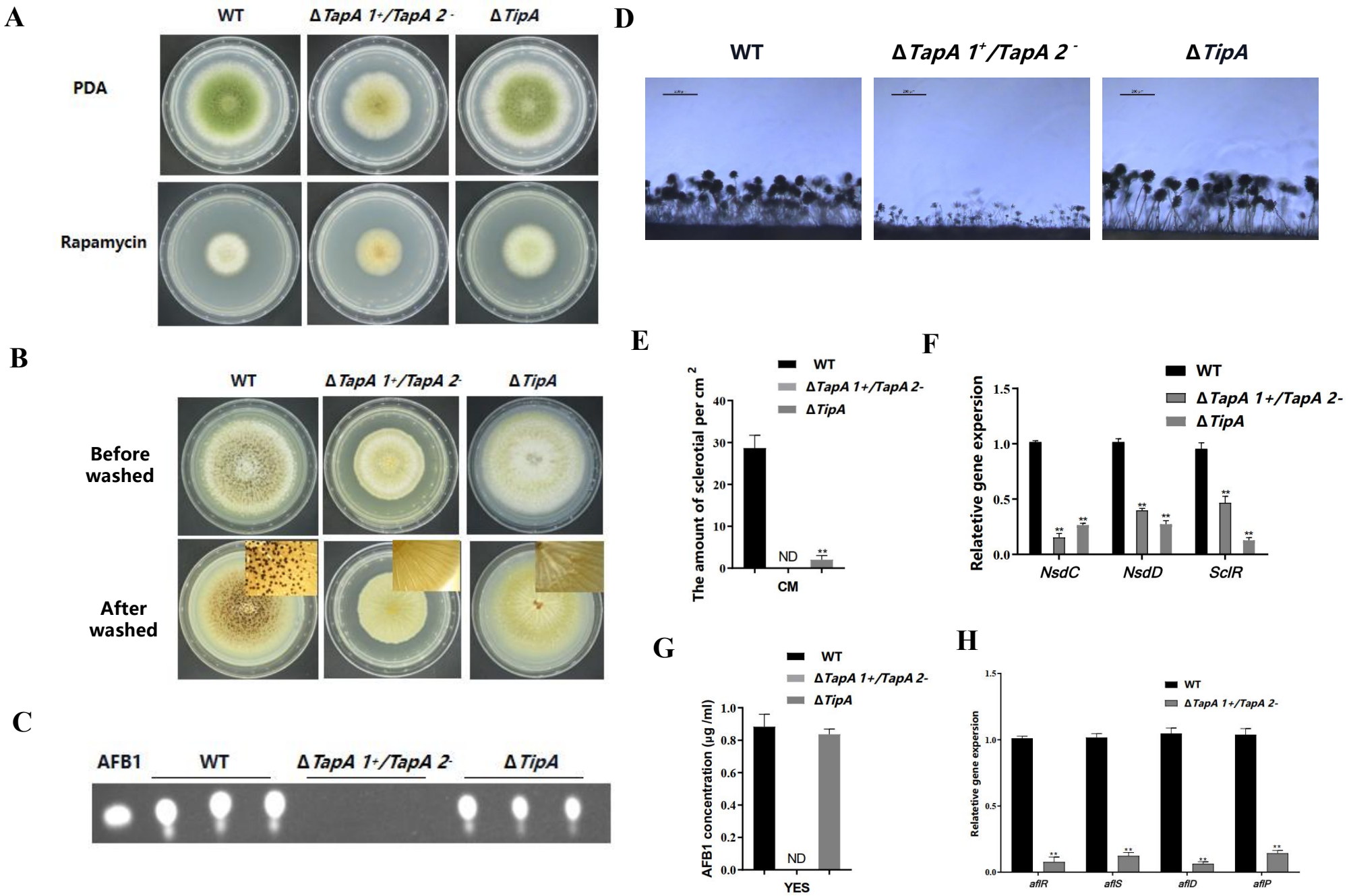
A
WT
ΔTapA 1+/TapA 2-
ΔTipA
PDA
Rapamycin
B
WT
ΔTapA 1+/TapA 2-
ΔTipA
Before washed
After washed
C
AFB1
WT
ΔTapA 1+/TapA 2-
ΔTipA
D
WT
ΔTapA 1+/TapA 2-
ΔTipA
E
WT
ΔTapA 1+/TapA 2-
ΔTipA
The amount of sclerotial per cm 2
ND
CM
F
WT
ΔTapA 1+/TapA 2-
ΔTipA
Relatetive gene expersion
NsdC
NsdD
SclR
G
WT
ΔTapA 1+/TapA 2-
ΔTipA
AFB1 concentration (μg /ml)
ND
YES
H
WT
ΔTapA 1+/TapA 2-
Relatetive gene expersion
aflR
aflS
aflD
aflP

Fig. 5 TapA and TipA regulate growth, sclerotia and aflatoxin biosynthesis in *A. flavus.*

(A) Phenotype of the *A. flavus* WT, Δ*TapA1*$^{+}$/*TapA*2^{-} and Δ*TipA* strains grown on PDA amended with 100 ng/mL rapamycin at 37°C for 5 days.

(B) Colony phenotype of the WT, Δ*TapA1*$^{+}$/*TapA*2^{-}and Δ*TipA* strains grown on CM medium at 37°C for 7 days.

(C) TLC assay of AFB_1 production by the WT, Δ*TapA1*$^{+}$/*TapA*2^{-} and Δ*TipA* strains cultured in YES liquid medium at 29°C for 6 days.

(D) Fluorescent images of hyphal cells for the WT, Δ*TapA1*$^{+}$/*TapA*2^{-} and Δ*TipA* strains stained with calcofluor white (CFW).

(E) Amounts of sclerotia produced by the WT, Δ*TapA1*$^{+}$/*TapA*2^{-} and Δ*TipA* strains.

(F) Relative transcript levels of sclerotia-related genes in WT and Δ*TapA1*$^{+}$/*TapA*2^{-}strains.

(G) Relative quantification of AFB1 production as in (C).

(H) Relative transcript levels of aflatoxin biosynthesis regulatory and structural genes in WT and Δ*TapA1*$^{+}$/*TapA*2^{-}strains.

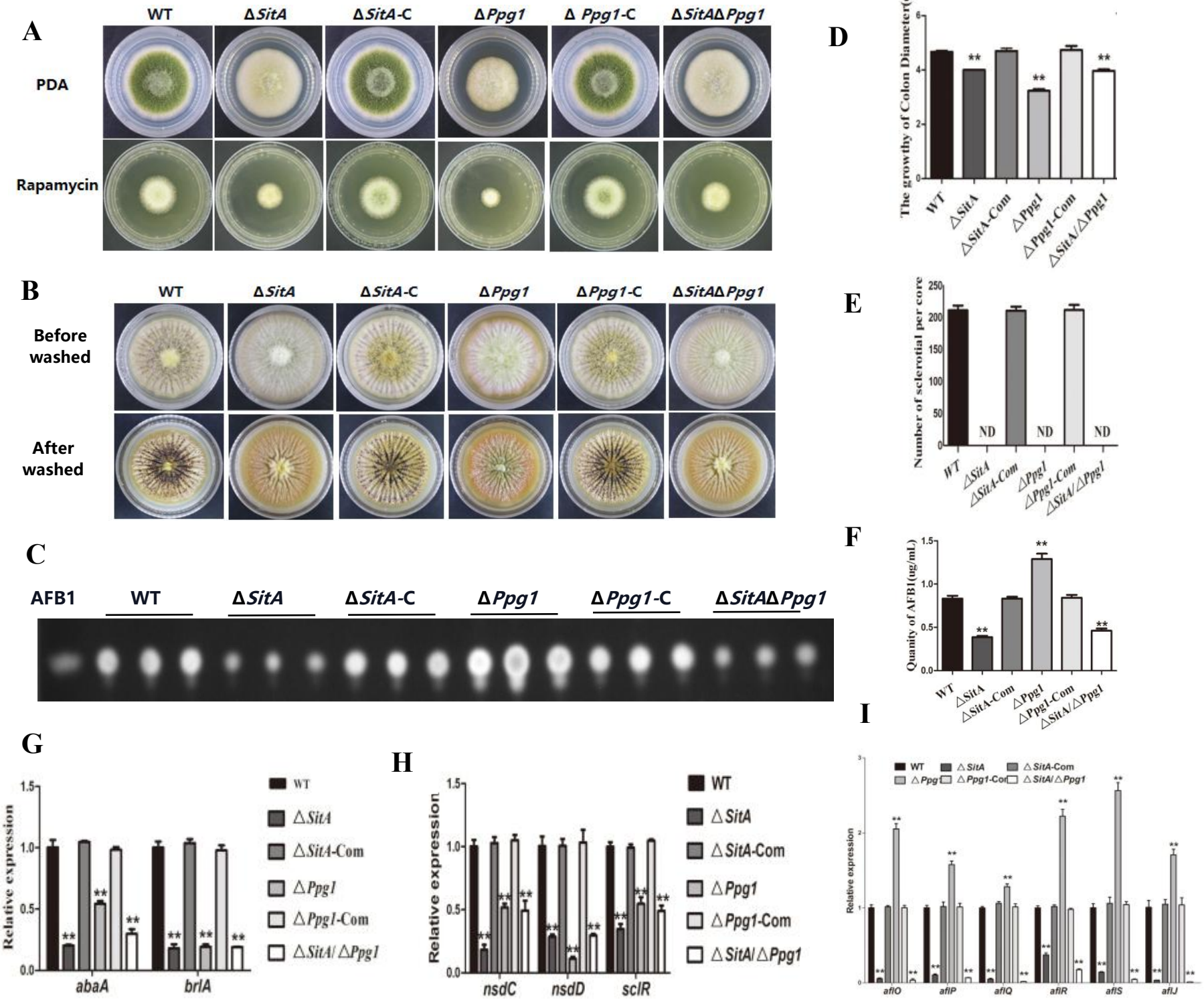
A
WT
ΔSitA
ΔSitA-C
ΔPpg1
Δ Ppg1-C
ΔSitAΔPpg1
PDA
Rapamycin
B
Before washed
After washed
C
AFB1
D
The growthy of Colon Diameter(
E
Number of sclerotial per core
ND
F
Quanity of AFB1(ug/mL)
G
Relative expression
abaA
brlA
H
nsdC
nsdD
sclR
I
aflO
aflP
aflQ
aflR
aflS
aflJ

Fig. 6 Phosphatases SitA and Ppg1 are involved in growth, conidiation and aflatoxin biosynthesis in *A. flavus.*

(A) The colony morphology of *A. flavus* WT, single knockout and double knockout strains of *SitA* and *Ppg1* cultured on PDA medium amended with 100 ng/mL rapamycin at 37°C for 5 days.

(B) The colony morphology of *A. flavus* WT, single knockout strain and double knockout strain of *SitA* and *Ppg1* cultured on WKM medium at 37°C for 7 days.

(C) TLC detection of WT, single knockout and double knockout strains of *SitA* and *Ppg1* cultured in YES liquid medium at 29°C for 6 days.

(D) Comparison of conidial production among WT, single knockout and double knockout strains on PDA media.

(E) Sclerotia statistics of WT, single knockout and double knockout strains.

(F) Quantitative analysis of AFB_1 of WT, single knockout and double knockout strains.

(G) Relative transcript levels of conidia synthesis genes in WT, single knockout and double knockout strains.

(H) Relative transcript levels of sclerotia synthesis genes in WT, single knockout and double knockout strains.

(I) Relative transcript levels of aflatoxin biosynthesis genes in WT, single knockout and double knockout strains.

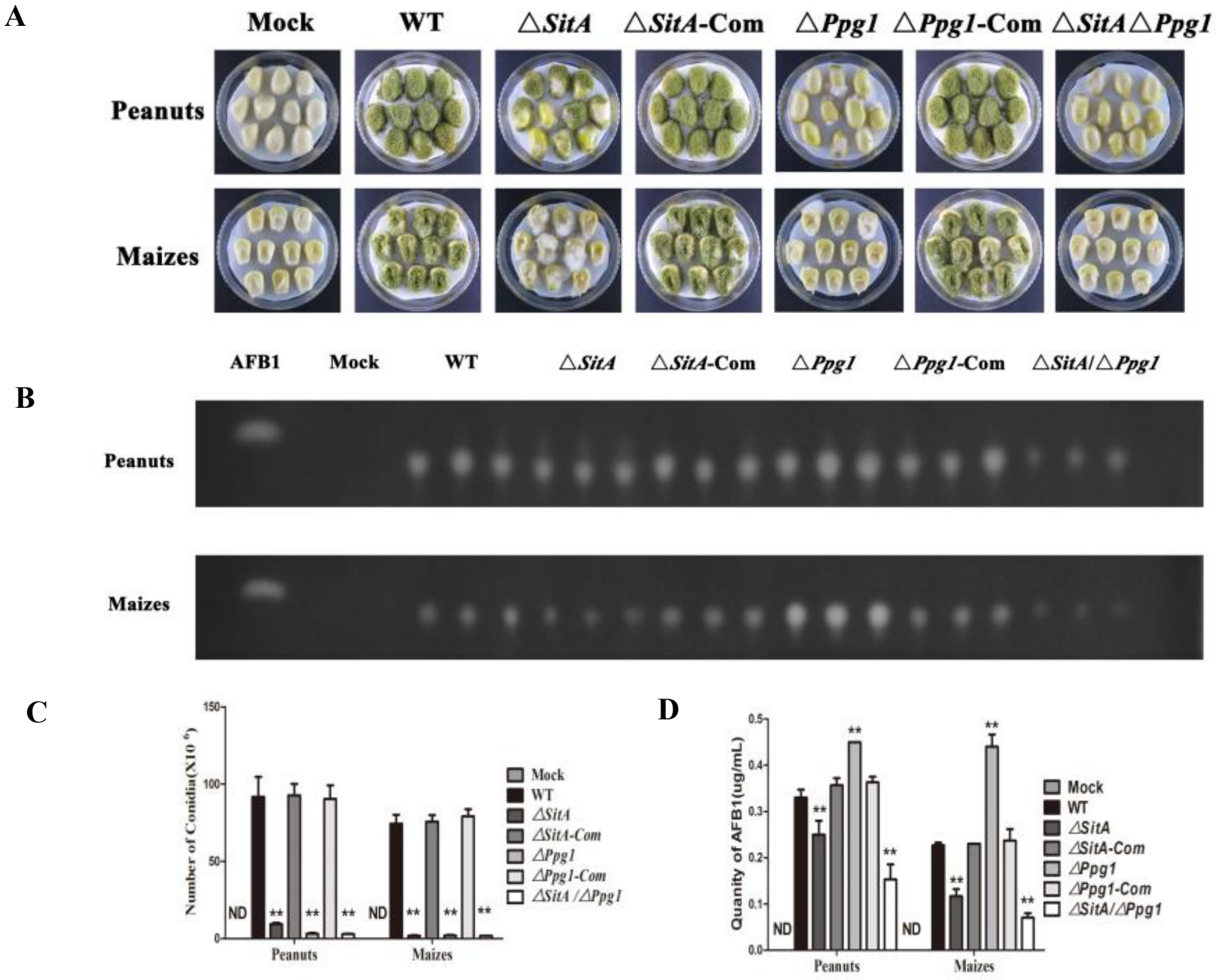
A
Mock
WT
△SitA
△SitA-Com
△Ppg1
△Ppg1-Com
△SitA△Ppg1
Peanuts
Maizes
B
AFB1
Mock
WT
△SitA
△SitA-Com
△Ppg1
△Ppg1-Com
△SitA/△Ppg1
Peanuts
Maizes
C
Number of Conidia(X10 6)
150
100
50
0
ND
**
Peanuts
Maizes
Mock
WT
△SitA
△SitA-Com
△Ppg1
△Ppg1-Com
△SitA /△Ppg1
D
Quanity of AFB1(ug/mL)
0.5
0.4
0.3
0.2
0.1
0.0
ND
**
Peanuts
Maizes
Mock
WT
△SitA
△SitA-Com
△Ppg1
△Ppg1-Com
△SitA/△Ppg1

Fig. 7 Phosphatase SitA and Ppg1 are important for pathogenicity in *A. flavus.*

(A) Phenotypes of peanut and maize infected by *A. flavus* WT, single and double knockout strains of *SitA* and *Ppg1*.

(B) TLC detection of toxin from peanut and maize infected by WT, single knockout and double knockout strains.

(C) Spores statistics from peanut and maize infected by WT, single and double knockout strains.

(D) Quantitative analysis of AFB_1 from peanut and maize infected by WT, single knockout and double knockout st

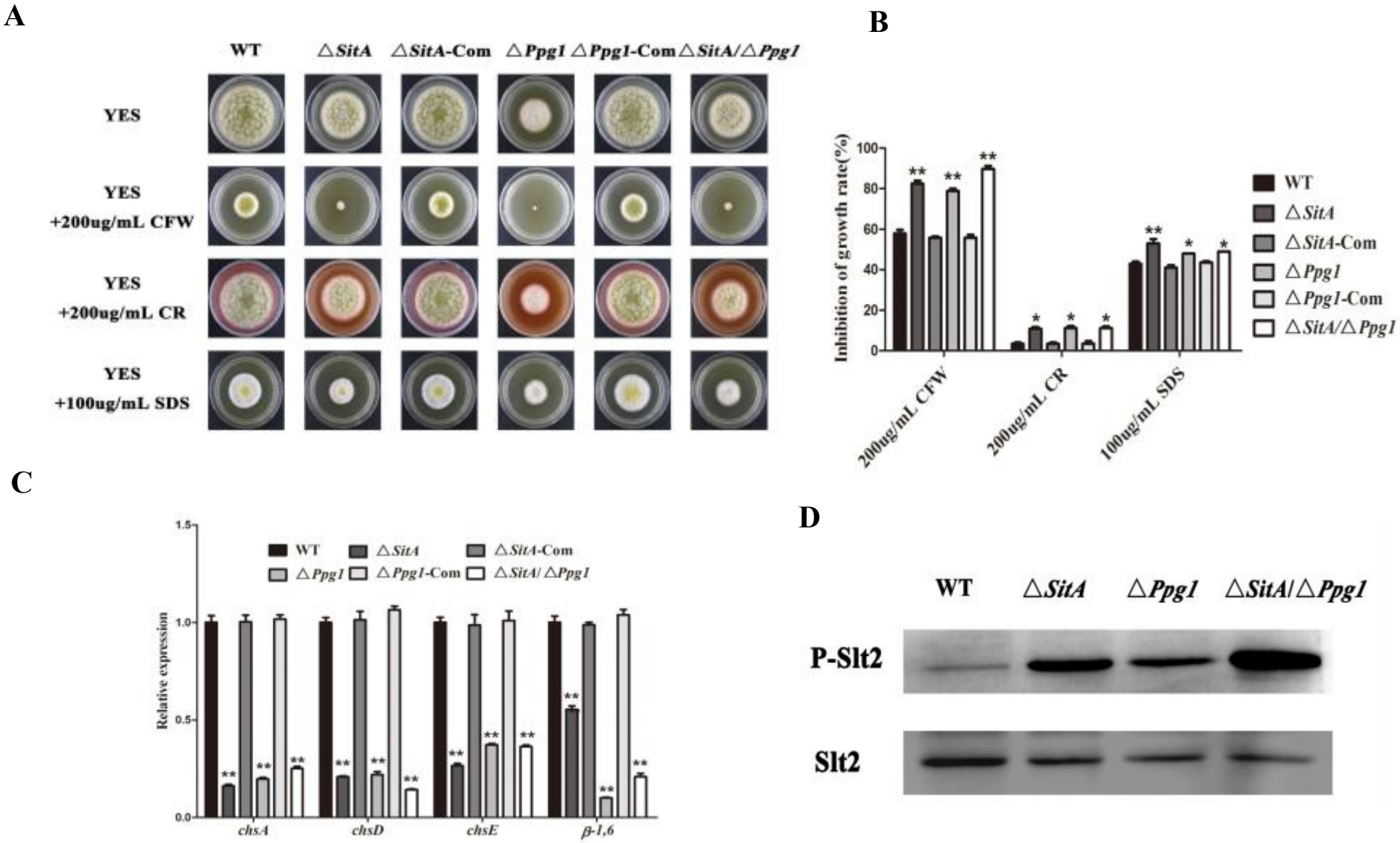
A
WT
△SitA
△SitA-Com
△Ppg1
△Ppg1-Com
△SitA/△Ppg1
YES
YES +200ug/mL CFW
YES +200ug/mL CR
YES +100ug/mL SDS
B
Inhibition of growth rate(%)
100
80
60
40
20
0
200ug/mL CFW
200ug/mL CR
100ug/mL SDS
WT
△SitA
△SitA-Com
△Ppg1
△Ppg1-Com
△SitA/△Ppg1
C
Relative expression
1.5
1.0
0.5
0.0
WT
△SitA
△SitA-Com
△Ppg1
△Ppg1-Com
△SitA/△Ppg1
chsA
chsD
chsE
β-1,6
D
WT
△SitA
△Ppg1
△SitA/△Ppg1
P-Slt2
Slt2

Fig. 8 Phosphatase SitA and Ppg1 are involved in regulating cell wall integrity.

(A) Morphology of *A. flavus* WT, single knockout and double knockout strains of *SitA* and *Ppg1* grown on PDA media supplemented with 200 μg/mL CR, 200 μg/mL CFW, or 100 μg/mL SDS at 37°C for 5 days.

(B) The growth inhibition rate of the WT, single knockout and double knockout strains under cell wall and cell membrane stress.

(C) Expression levels of cell wall synthesis genes (*chsA*, *chsD*, *chsE* and *β-1,6*) in WT, single knockout and double knockout strains.

(D) Phosphorylation level of Slt2 in WT, single knockout and double knockout strains was detected by Western blotting.

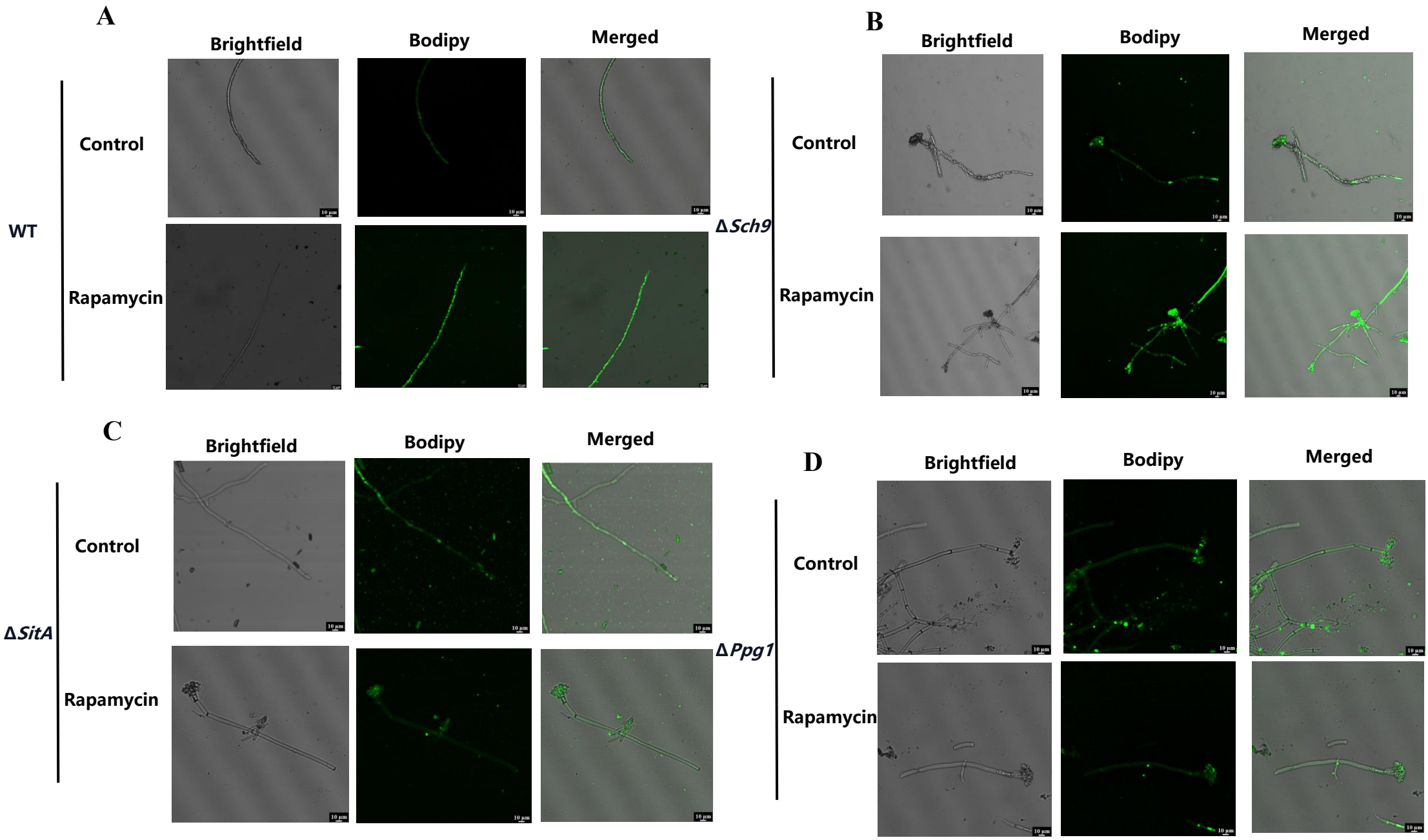
A
Brightfield
Bodipy
Merged
WT
Control
Rapamycin
B
Brightfield
Bodipy
Merged
ΔSch9
Control
Rapamycin
C
Brightfield
Bodipy
Merged
ΔSitA
Control
Rapamycin
D
Brightfield
Bodipy
Merged
ΔPpg1
Control
Rapamycin

Fig. 9 Phosphatase SitA and Ppg1 are involved in regulating lipid droplet biogenesis.

(A) The intracellular lipid droplets were stained by boron dipyrromethene difluoride (BODIPY) in hyphae of the *A. flavus* WT strain and observed under a fluorescence microscopy. The Phenotype of lipid droplets accumulation in the mycelia of *A. flavus* WT strain treated with or without 100 ng/mL rapamycin cultured for 6 h. Bar, 10 μm.

(B) The phenotype of lipid droplets accumulation in the mycelia of Δ*Sch9* strain treated with or without 100 ng/mL rapamycin cultured for 6 h.Bar, 10 μm.

(C) The phenotype of lipid droplets accumulation in the mycelia of Δ*SitA* strain treated with or without 100 ng/mL rapamycin cultured for 6 h.Bar, 10 μm.

(D) The phenotype of lipid droplets accumulation in the mycelia of Δ*Ppg1* strain treated with or without 100 ng/mL rapamycin cultured for 6 h. Bar, 10 μm.

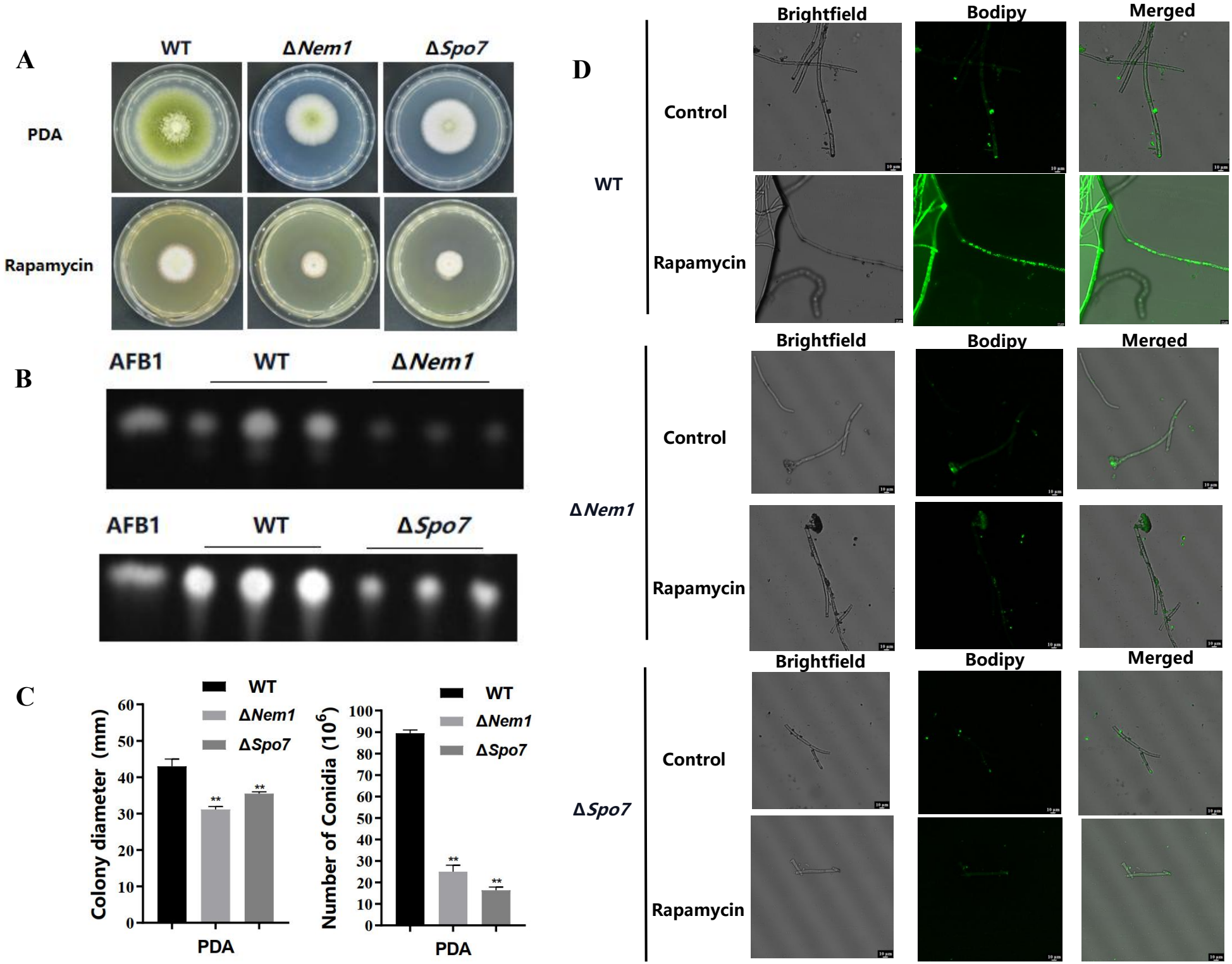
A
WT
ΔNem1
ΔSpo7
PDA
Rapamycin
B
AFB1
WT
ΔNem1
AFB1
WT
ΔSpo7
C
WT
ΔNem1
ΔSpo7
Colony diameter (mm)
60
50
40
30
20
10
0
**
**
PDA
WT
ΔNem1
ΔSpo7
Number of Conidia (10^6)
100
90
80
70
60
50
40
30
20
10
0
**
**
PDA
D
Brightfield
Bodipy
Merged
Control
WT
Rapamycin
Brightfield
Bodipy
Merged
Control
ΔNem1
Rapamycin
Brightfield
Bodipy
Merged
Control
ΔSpo7
Rapamycin

Fig. 10 Phosphatase complex Nem1/Spo7 play an important role in growth, conidiation and aflatoxin and lipid droplet biogenesis.

(A) Phenotype of the *A. flavus* WT, Δ*Nem1* and Δ*Spo7* strains grown on PDA amended with 100 ng/mL rapamycin at 37°C for 5 days.

(B) TLC assay of AFB_1 production by the *A. flavus* WT, Δ*Nem1* and Δ*Spo7* strains cultured in YES liquid medium at 29°C for 6 days.

(C) Statistical analysis of the diameter and sporulation by the *A. flavus* WT, Δ*Nem1* and Δ*Spo7* strains.

(D) The Phenotype of lipid droplets accumulation in the mycelia of the *A. flavus* WT, Δ*Nem1* and Δ*Spo7* strains treated with or without 100 ng/mL rapamycin cultured for 6 h. Bar, 10 μm.

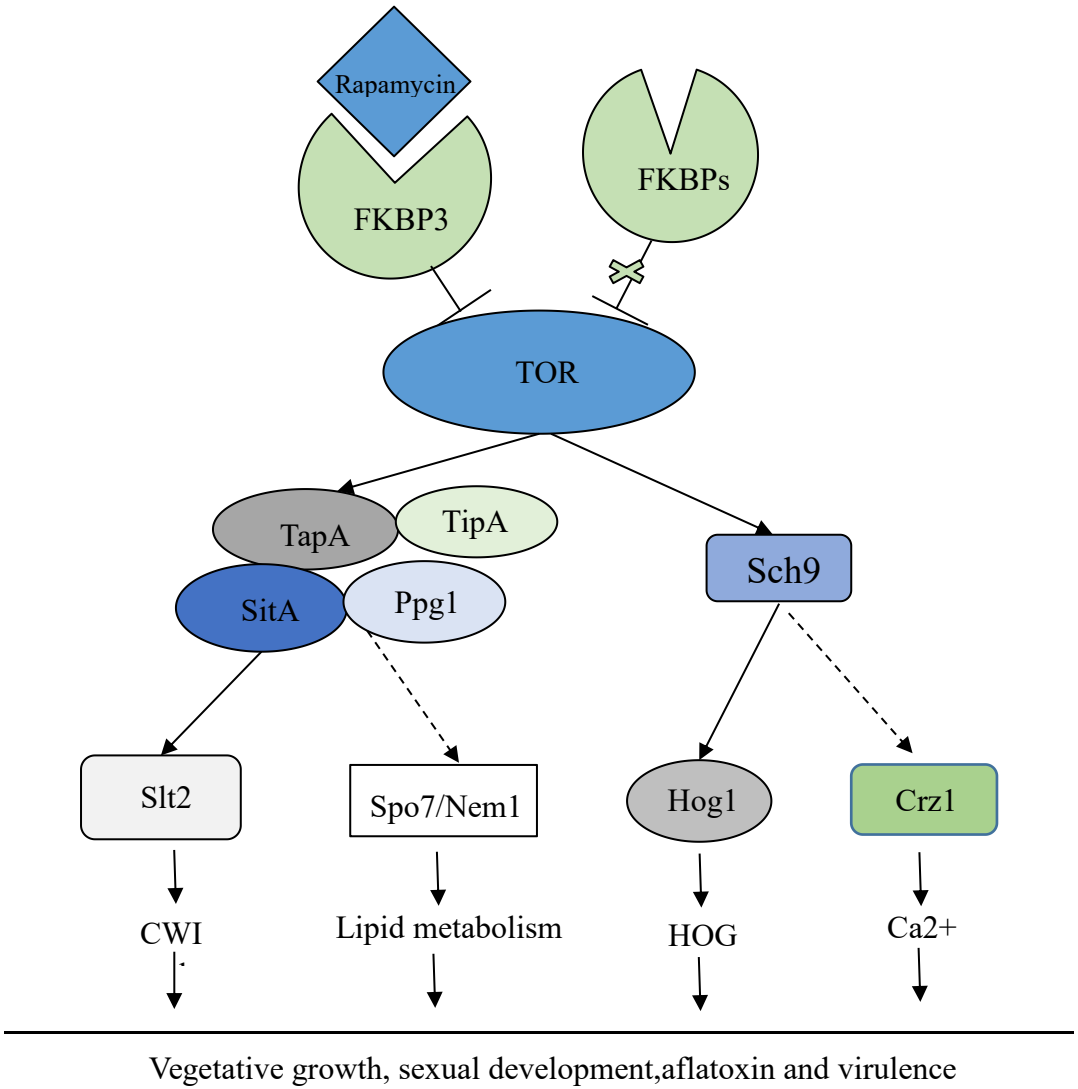
Rapamycin
FKBP3
FKBPs
TOR
TapA
TipA
SitA
Ppg1
Sch9
Slt2
Spo7/Nem1
Hog1
Crz1
CWI
Lipid metabolism
HOG
Ca2+
Vegetative growth, sexual development,aflatoxin and virulence

Fig. 11 The proposed model of target of the rapamycin (TOR) pathway in *A. flavus*.

Based on the above results, we hypothesized the TOR signaling pathway model in *A. flavus.* Rapamycin forms a complex with FKBP3, and this complex can bind to the Tor kinase to inhibit its normal function. Sch9 as a downstream component of the Tor kinase, regulates sclerotia formation, aflatoxin biosynthesis, the TOR and HOG signaling pathways. In addition, We speculate that the Sch9 as a element for the calcineurin-CrzA pathway in response to calcium stress. As another important target of the Tor kinase, Tap42-phosphatase complex is involved in the regulation of growth, sporulation, sclerotia, aflatoxin production, CWI signaling pathways, lipid droplet synthesis and other processes. In conclusion, the TOR signaling pathway plays an important role in the vegetative development, stress responses, aflatoxin biosynthesis and pathogenicity in *A. flavus.*